HAL
open science

ADAM17/TACE inhibits Schwann cell myelination

Rosa La Marca, Federica Cerri, Keisuke Horiuchi, Angela Bachi, Maria Laura Feltri, Lawrence Wrabetz, Carl P. Blobel, Angelo Quattrini, James L. Salzer, Carla Taveggia

To cite this version:

Rosa La Marca, Federica Cerri, Keisuke Horiuchi, Angela Bachi, Maria Laura Feltri, et al.. ADAM17/TACE inhibits Schwann cell myelination. Nature Neuroscience, 2011, 10.1038/nn.2849 . hal-00650655

HAL Id: hal-00650655

https://hal.science/hal-00650655v1

Submitted on 12 Dec 2011

HAL is a multi-disciplinary open access archive for the deposit and dissemination of scientific research documents, whether they are published or not. The documents may come from teaching and research institutions in France or abroad, or from public or private research centers.

L'archive ouverte pluridisciplinaire **HAL**, est destinée au dépôt et à la diffusion de documents scientifiques de niveau recherche, publiés ou non, émanant des établissements d'enseignement et de recherche français ou étrangers, des laboratoires publics ou privés.

FONDAZIONE CENTRO SAN RAFFAELE DEL MONTE TABOR

ISTITUTO DI RICOVERO E CURA A CARATTERE SCIENTIFICO

Milan, April 7, 2011

Kalyani Narasimhan, Ph.D.
Chief Editor
Nature Neuroscience

Dear Dr Narasimhan,

We are enclosing our revised manuscript entitled "ADAM17/TACE inhibits Schwann cell myelination". We have changed the manuscript following the requested editorial change.

We have shortened the manuscript and now the main body is less than 5000 words and the Material and Method section less than 2000. As requested we have also reduced the total number of references and modified the Figures. We have added one Supplementary Figure that contains the un-cropped version of the Western Blots presented in the manuscript.

Together with the manuscript and the main figures in TIFF format, we have upoloaded a pdf document containing all the supplementary information (Figures and Table), the License to publish, the SI guide and the Nature Neuroscience checklist guide.

We would like to take this opportunity to thank *Nature Neuroscience* for the interest in our work.

Yours Sincerely,

Carla Taveggia

H SAN RAFFAELE

Via Olgettina 60 • 20132 Milano Italy • Tel. 022643.1 • Cod. Fisc. 03064280153

ADAM17/TACE inhibits Schwann cell myelination

Rosa La Marca[1,2], Federica Cerri[1,2], Keisuke Horiuchi[3], Angela Bachi[4], M. Laura Feltri[4], Lawrence Wrabetz[4], Carl P. Blobel[5], Angelo Quattrini[1,2], James L. Salzer[6,7,8] and Carla Taveggia[1,2,#]

[1]Division of Neuroscience, [2]INSPE and [4]Division of Genetics and Cell Biology at San Raffaele Scientific Institute, 20132 Milan, Italy; [3]Department of Orthopedic Surgery, School of Medicine, Keio University, Tokyo 160-8582, Japan; [5]Arthritis and Tissue Degeneration Program, Hospital for Special Surgery at Weill Medical College of Cornell University, New York, NY 10021, USA; Departments of [6]Cell Biology, [7]Neurology, and [8]Smilow Neuroscience Program, NYU School of Medicine, 10016, New York, NY, US.

To whom correspondence should be addressed. E-mail:taveggia.carla@hsr.it

running title: TACE in myelination

SUMMARY

TACE, the tumor necrosis factor alpha–converting enzyme, is a proteolytic sheddase responsible for the cleavage of several membrane-bound molecules. We report that TACE cleaves NRG1 type III in the EGF domain, likely inactivating it, as assessed by deficient activation of PI–3 kinase pathway, thereby negatively regulating PNS myelination. Lentiviral mediated knockdown of TACE *in vitro* in dorsal root ganglia neurons accelerates the onset of myelination and results in hypermyelination. In agreement, conditional knockout mice lacking TACE in motor neurons are significantly hypermyelinated and small caliber fibers aberrantly myelinated. Further, reduced TACE activity rescues NRG1 type III hypomyelination *in vivo*. We also show that the inhibitory effect of TACE is neuron autonomous as Schwann cells lacking TACE elaborate myelin of normal myelin thickness. Thus, TACE is a novel modulator of Neuregulin 1 type III activity and is a significantly negative regulator of myelination in the PNS.

Myelin, the insulating membrane produced by Schwann cells in the peripheral nervous system (PNS) and oligodendrocytes in the central nervous system (CNS), is a remarkable organelle whose assembly and function is crucial for proper transmission of the electric impulse. Myelination in the PNS is controlled at the molecular level by the amount of axonal Neuregulin 1 (NRG1) type III [1, 2]. Thus, clarifying the mechanisms controlling NRG1 type III expression is essential to establish the molecular events regulating myelin formation. The β–secretase BACE1 [3-5] and the α–secretases belonging to the ADAM family of proteases [6] control NRG1 classical regulated proteolysis. While the role of BACE1 in NRG1 type III cleavage has been investigated during myelination and remyelination [3-5], the role of α–secretases is unclear.

ADAMs (a disintegrin and metalloprotease) are a family of zinc–dependent membrane–anchored metalloproteases implicated in ectodomain shedding of several growth factors. These proteins control myogenesis, neurogenesis, fertilization, inflammation and myelination[6]. Several members of the ADAM secretases are expressed in the PNS and some have been implicated in myelination. In particular ADAM 19 can process NRG1 [7], although recent studies suggest that ADAM 19 targets NRG1 type I [8], which is not implicated in myelination[1, 2]. Accordingly, mice lacking ADAM 19 myelinate normally although they have delayed remyelination [9]. Another ADAM directly implicated in myelination is ADAM 22 as transgenic animals lacking ADAM 22 are hypomyelinated in the PNS [10]. However it is unlikely that ADAM 22 cleaves NRG1 type III or other growth factors since this protein lacks a catalytic site consensus sequence [6]. Rather, axonal ADAM 22 functions as a receptor for secreted Lgi4 proteins [11]. Recently the role of ADAM 10 in NRG1 cleavage has been analyzed. Animals with altered ADAM 10 expression however myelinate normally in the PNS[12] suggesting that ADAM 10 is dispensable.

Another member of this family, ADAM 17 also known as TACE (TNF– α converting enzyme), has been implicated in NRG1 cleavage [13]. TACE mediates ectodomain shedding of several membrane–bound molecules, including TNF– α, TGF–α, $p75^{NTR}$, Notch and APP[6, 14] in addition to NRG1. Animals lacking TACE die at birth, preventing the analyses of myelination *in vivo* [15]. We now report that TACE cleaves NRG1 type III and that ablation of TACE results in altered processing of axonal NRG1

type III. In addition, downregulation of TACE expression *in vitro* in myelinating cocultures and *in vivo* inactivation of TACE in motor neurons leads to precocious myelination, hypermyelination, ectopic myelination and enhanced activation of the PI–3K pathway. Furthermore, reduction of TACE activity *in vivo* is sufficient to rescue myelination of NRG1 type III haploinsufficient mice. We also provide evidences that this phenotype is due to a cell autonomous mechanism, as inactivation of TACE in Schwann cells *in vitro* and *in vivo* does not alter the timing or amount of the myelin produced.

Thus, our study reveals a novel role of TACE in myelination. By cleaving NRG1 type III, TACE determines the amount of this critical regulator of myelination on the axonal surface and, unlike BACE1[3, 5], negatively regulates PNS myelination. To our knowledge this is the first study reporting a negative mechanism for controlling NRG1 type III expression and myelination, further suggesting secretases are important modulators of myelination.

RESULTS

TACE inactivation enhances myelination in vitro

To investigate the role of TACE in myelination we first analyzed its mRNA and protein levels *in vitro*. TACE is highly expressed in Schwann cells and, at lower levels, in dorsal root ganglia (DRG) neurons as shown by RT–PCR and Western blotting analyses of cDNAs or lysates prepared from Schwann cells and DRG neurons (**Supplementary Fig. 1**).

TACE$^{-/-}$ animals die at birth [15], precluding *in vivo* analysis of myelination. To determine the role of TACE in myelin formation, we first knocked down its expression using specific shRNA lentiviruses. For our studies we have used three different shRNA clones (TRCN0000031949, TRCN0000031952 and TRCN0000031953) obtained from the siRNA Consortium (Boston, MA, US) together with a lentiviral vector expressing a scrambled artificial sequence as a negative control. BLAST analyses confirmed that the sequence used in the scrambled shRNA did not recognize any mammalian DNA. To validate the specificity of *TACE* shRNAs, we tested their capability to modulate p75^{NTR} and Notch–1 cleavage. Both molecules are important in myelination [16, 17], but only p75^{NTR} is cleaved by TACE [18], whereas Notch–1 is extracellularly processed by ADAM 10 [19, 20]. As expected we have observed impaired p75^{NTR} cleavage in cocultures infected with *shTACE* lentiviruses, but not altered levels of Notch–1 intracellular domain (NICD) (**Supplementary Fig. 2**).

To corroborate the efficacy of knockdown we infected primary rat Schwann cells for 2 days and then analyzed expression by Western Blotting on an Odyssey imaging system (**Fig. 1a**). All the three tested shRNAs significantly decrease TACE expression by approximately 80% when compared to mock–infected or control uninfected Schwann cells (**Fig. 1b**). We then infected mouse DRG explant cultures, which contain a mix of Schwann cells and DRG neurons, with lentiviruses encoding *TACE* or scramble shRNAs for 48 hours. The cultures were grown without antimitotic agents to allow infection of both neurons and Schwann cells. Western Blotting analysis confirmed effective TACE knockdown of infected cultures (data not shown). Myelination was induced by supplementing the cultures with 50 μg/ml ascorbic acid. Immunofluorescence analysis

(**Fig. 1e**) for myelin basic protein (*MBP*) and neurofilament showed that myelination was significantly increased in *shTACE* infected cultures, and was already substantial 3 days after ascorbic acid addition. Thus, myelination in cocultures infected with *shTACE* was strongly enhanced and commenced earlier when compared to scramble infected or control not infected cultures, suggesting that *TACE* inhibits myelination. To further confirm this result we have counted the number of MBP^+ segments 3 days after ascorbic acid addition, in *shTACE* infected versus not infected or scramble infected cultures. Specific knock down of *TACE* leads to an approximately 15–fold increase in myelination (**Fig 1c**). Western blotting analyses for myelin proteins confirmed the hypermyelination. Myelin Protein Zero (*MPZ*) is significantly upregulated in cocultures infected with *shTACE* lentiviruses 14 days after induction of myelination (**Fig. 1d**).

Since *TACE* knock down determines enhanced and precocious myelination, our data suggest that *TACE* might control the temporal activation of the myelinating program.

TACE activity in vitro is neuronal cell autonomous

These results indicate that *TACE* negatively controls myelination. As both Schwann cells and DRG neurons express *TACE*, we sought to determine whether *TACE* effects are specific to Schwann cells, to neurons or both using a purified myelinating coculture system. We first infected murine DRG neurons with *shTACE* lentiviruses or, as control, with the shscr lentiviral supernatant. We then cocultured them with primary not infected rat Schwann cells and induced myelination for 15 days by ascorbic acid addition; cultures were then stained for MBP and neurofilament. DRG neurons knocked down for *TACE* are substantially hypermyelinated (**Fig. 2a** sh1, **Supplementary Fig. 3a** sh2, sh3). The number of myelinated segments in neurons lacking *TACE* is increased approximately 8–fold (**Fig. 2b**). As in the previous experiment, we did not observe any effect on neurite outgrowth. We confirmed these results by Western Blotting analyses of MBP, MAG and neurofilament expression. As expected, myelin proteins expression is significantly upregulated in lysates of cocultures ablated in neuronal *TACE* (data not shown).

In a parallel set of experiments, we inactivated *TACE* in rat primary Schwann cells and cocultured them with purified uninfected mouse DRG neurons. Cultures were maintained in myelinating condition for 21 days. Immunofluorescence for MBP and neurofilament (**Fig. 2c** sh1, **Supplementary Fig. 3b** sh2, sh3) and Western Blot analyses

for MBP and MAG (data not shown) indicate that inactivation of *TACE* in Schwann cells does not enhance myelination, strongly suggesting that the inhibitory role of *TACE* in myelination is neuronal cell autonomous. These results were further confirmed by assessing numbers of MBP^+ segments in these cultures, which were comparable between TACE knockdown and control cultures (**Fig. 2d**).

Thus, these studies indicate that TACE acts in a neuron autonomous fashion to inhibit myelination in an *in vitro* model of PNS myelination.

In vivo inactivation of axonal TACE leads to hypermyelination

To evaluate the role of *TACE* in myelination during development and to determine whether neuronal *TACE* also inhibits myelination *in vivo*, we have generated transgenic mice lacking TACE specifically in motor neurons. To this end, we crossed mice containing LoxP sites flanking exon 2 of *TACE* ($TACE^{flx/flx}$) [21] with the *HB9–Cre* transgenic line, which has been used in previous studies to drive motor neuron-specific recombination[22]. We screened the genotype by PCR analysis on genomic DNA prepared from tail and spinal cord of $HB9Cre//TACE^{flx/flx}$ and wild type controls (data not shown). Since the *HB9–Cre* transgenic line is expressed in motor neurons we have corroborated efficient recombination by determining TACE mRNA expression by RT–PCR on spinal cord of $HB9Cre//TACE^{flx/flx}$ and *wild type* mice (**Fig. 3a**) and TACE protein levels in lysates prepared from P30 wild type and null femoral nerves (**Fig. 3b**). *TACE* expression is reduced both at mRNA and protein levels in null animals. Residual expression is likely due to non–recombined TACE present in other cells; in femoral nerves mainly Schwann cells and sensory nerve fibers.

Ultrastructure analysis of the ventral roots and sciatic nerves from newborn (P1) $HB9Cre//TACE^{flx/flx}$ showed that the onset of myelination in ventral roots of null animals was accelerated (**Fig. 3c**). As expected we have observed that some fibers in P1 sciatic nerves, which contain both sensory and motor fibers, are hypermyelinated (**Fig. 3d**). Quantitation of the number of myelinated fibers demonstrated a significant increase in null mice; the total number of nerve fibers was similar in both genotypes (**Table 1**).

To evaluate whether the hypermyelination of $HB9Cre//TACE^{flx/flx}$ mice is maintained during active phases of myelination, we analyzed peripheral nerve

morphology in P7 and P15 sciatic nerves. At both time points neurites were hypermyelinated as evidenced in semithin sections (**Fig. 4a–b**, top panels) and in electron micrographs (**Fig. 4a–b**, lower panels). The hypermyelinating phenotype has also been confirmed by *g* ratio (axon diameter/fiber diameter) measurements (**Fig. 4c**), which is significantly decreased in P7 fibers of sciatic nerves of null animals (**Table 1**). This change does not result in alterations of fiber's diameters in null mice, which is similar to wild type (**Fig. 4d**) strongly suggesting that the observed phenotype is due to changes in the myelin sheath. As suggested from our previous data, hypermyelination in *HB9Cre//TACE*$^{flx/flx}$ mice determines a remarkable increase in the number of myelin lamellae surrounding fibers of similar caliber, with no alteration of myelin periodicity (**Fig. 4e**).

Morphological and ultrastructural analyses of P30 *HB9Cre//TACE*$^{flx/flx}$ ventral roots (**Fig. 5a**) and sciatic nerves (**Fig. 5b**) and *g* ratio measurements in sciatic nerves (**Fig. 5f** and **Table 1**), confirmed hypermyelination in adult mice, strongly suggesting that this effect is maintained throughout development. Surprisingly, we have observed a significant number of myelinated fibers with axons less than 1 μm in diameter and a remarkable reduction in the axonal diameters of myelinated fibers in sciatic nerves of null animals, despite the total number of myelinated fibers being similar between genotypes (*wild type*: 1717; *HB9Cre//TACE*$^{flx/flx}$: 1697) (**Fig. 5g** and **Table 1**). Whether this difference is due to ectopic myelination or constriction of axonal caliber will require further investigation. Nonetheless, this alteration is unlikely to explain the hypermyelination as both *in vitro* and *in vivo* studies indicate that the axonal diameter increases with myelin formation [23, 24]. Of note, we have similarly observed myelin sheath surrounding several fibers whose diameter is less than 1 μm also in ventral roots of null animals (**Fig. 5a**, asterisks). To determine whether the myelin protein content parallels the hypermyelinating phenotype we have checked MBP expression in P15 and P30 femoral nerves of wild type and null animals by Western Blotting analyses. As expected, hypermyelination is accompanied by increased MBP expression (**Fig. 5c**). Of note, even p–AKT levels (**Fig. 5d**), a key effector of the PI 3–kinase pathway, which acts downstream of NRG1 type III [1] and is important for PNS myelination [25, 26], are increased in P30 null femoral nerves.

Our ultrastructure analyses also revealed that ablation of neuronal *TACE* alters the organization of C fibers, engulfed by non–myelinating Schwann cells in Remak bundles. We have in fact observed unsorted and unmyelinated fibers, larger than 1 μm in diameter in $TACE^{-/-}$ Remak fiber (**Fig. 5e** asterisks), suggesting an impaired sorting process. Furthermore, in many cases Remak bundles lacked intervening Schwann cells processes, suggesting that TACE affects also the ensheathment process of non myelinated fibers.

To test whether TACE haploinsufficiency induces hypermyelination we have generated a complete $TACE^{-/-}$ transgenic line by crossing $TACE^{flx/flx}$ mice with *CMV–Cre* transgenic mice that allows recombination in all cells [27]. Morphological analyses, *g* ratio measurements and Western Blotting analyses for myelin proteins, show that $TACE^{+/-}$ P30 sciatic nerves are normally myelinated, indicating that residual TACE activity is sufficient to regulate myelin formation (**Supplementary Fig. S4** and **Table 1**).

Only axonal TACE determines hypermyelination

To corroborate our previous results, which indicate that hypermyelination is due to a neuron cell autonomy mechanism, we deleted *TACE* in Schwann cells, *in vivo*. Thus, we crossed *TACE* floxed transgenic animals with a *P0–Cre* transgenic line ($P0Cre//TACE^{flx/flx}$)[28]. We confirmed efficient recombination on genomic DNA of P15 sciatic nerves of $P0Cre//TACE^{flx/flx}$ mice by PCR analysis (**Fig. 6a**). Myelination in P7 and P30 $P0Cre//TACE^{flx/flx}$ sciatic nerves is similar to that of *wild type* control animals, as assessed by semithin sections (**Fig. 6b–c** top panels) and ultrastructural analyses (**Fig. 6b–c** lower panels). This result was further confirmed by *g* ratio measurements (**Fig. 6e**), which is not significantly different in *wild type* and *null* animals (**Table 1**). Furthermore, MBP and MAG protein levels are similar in *wild type* and *null* P15 sciatic nerves lysates (**Fig. 6d**). Surprisingly, despite similar numbers of myelinated fibers in wild type and $P0Cre//TACE^{flx/flx}$ mice (*wild type*: 1298; $P0Cre//TACE^{flx/flx}$: 1244), axonal diameters are slightly increased in $P0Cre//TACE^{flx/flx}$ sciatic nerves (**Fig. 6f** and **Table 1**). Furthermore, $P0Cre//TACE^{flx/flx}$ myelinated fibers have increased periaxonal space and accumulation of organelles in the inner cytoplasmic collar (**Supplementary Fig. 5**), suggesting that glial *TACE* may process molecules, which are implicated in myelin compaction and/or adhesion.

Taken together these *in vivo* analyses provide compelling evidence that neuronal *TACE* inhibits myelination in a neuron–cell autonomous mechanism. Ablation of *TACE* in motor neurons accelerates the myelinating process and results in hypermyelination, leading to an increase in the number of myelin lamellae of fibers with similar caliber, and ectopic myelination of small caliber fibers that would normally be unmyelinated. In addition our findings indicate that glial *TACE* also participates in the myelinating process, although it does not regulate myelin thickness.

TACE cleaves NRG1 and controls axonal type III NRG1 levels

The phenotype observed in *HB9Cre//TACE*$^{flx/flx}$ mice and particularly the increased number of myelin lamellae *in vivo* strongly resembles the hypermyelinating phenotype of *NRG1 type III* overexpressing mice [2]. In addition ablation of *TACE* is sufficient to determine myelination of fibers that would normally be amyelinated, mirroring what happens with ectopic expression of *NRG1 type III* [1]. Thus, by cleaving *NRG1* [13] *TACE* might regulate the amount of axonal NRG1 type III and hence PNS myelination. To determine whether NRG1 shedding is altered in the absence of *TACE* we have analyzed NRG1 expression in lysates of *wild type*, *TACE*$^{+/-}$and *TACE*$^{-/-}$ DRG neurons prepared from E14.5 embryos (**Fig. 7a**), and of P30 *HB9Cre//TACE*$^{flx/flx}$ femoral nerves (**Fig. 7b**). In the absence of *TACE*, NRG1 processing is impaired as levels of the unprocessed pro–protein form are increased in DRG null neurons. Interestingly, full length NRG1 pro–protein is absent in *TACE* null femoral nerves, and barely present in *wild type* control extracts. This difference is likely due to altered NRG1 expression in DRG neurons in culture and in sciatic nerves [1]. More importantly, levels of cleaved NRG1 are similarly increased in the absence of *TACE*, probably due to enhanced activity of other secretases (i.e. BACE1).

To further confirm these data, we have mapped the TACE cleavage site of NRG1 by mass spectrometry analyses. Hence, we have incubated 2 μg of human recombinant NRG1 β1 with 1 μg of human recombinant TACE. The proteins were then separated on a Tris-Tricine gel to favor the resolution of small molecular weight bands together with native uncleaved recombinant NRG1 β1 protein for comparison (**Fig. 7c**). This reaction generates a cleavage product of ~6 KDa (**Fig. 7c** arrow), which was digested with Endoproteinase Glu-C and analyzed by MALDI-TOF mass spectrometry. In the MALDI-

TOF spectrum two potential C-terminal peptides were detected that did not correspond to Endoproteinase Glu-C cleavage (**Supplementary Fig. 6**) and should therefore derive from TACE activity (**Fig. 7d**). These peptides with mass of 1858.812 Da and 2294.057 Da correspond to the peptide sequences FTGDRCQNYVMASFY and FTGDRCQNYVMASFYKHLG respectively, suggesting that TACE cleaves NRG1 β1 either upstream or in the β exon of the EGF domain 3/6 amino-acids before the previously identified BACE1 site (**Fig. 7e**)[4]. In our analysis we never observed the BACE1 cleavage site of NRG1.

To determine whether following TACE cleavage, the activity of NRG1 type III is altered, we have incubated control *wild type* and *TACE*$^{-/-}$ DRG neurons with chimeric erbB2/erbB3 protein; this molecule, fused to the Fc portion of human IgG (erbB2/B3–Fc) binds to NRG1 type III molecules, the only NRG1 expressed on the axonal surface[1]. Chimeric erbB2/B3–Fc protein binds more robustly to DRG neurons lacking TACE compared to wild type uninfected or control shRNA infected DRG neurons (**Fig. 7f**). Similar results were obtained in DRG neurons in which *TACE* expression has been ablated by shRNA infection (**Supplementary Fig. 7**). Inhibition of *TACE* results in approximately 50 % increase in NRG1 type III expressed on the axonal surface (**Fig. 7g**).

These results confirm that TACE cleaves NRG1 and suggest that TACE might inhibit myelination by limiting the levels of functional NRG1 type III on the axonal surface.

TACE alters NRG1 type III signaling and myelination

Despite the key role of NRG1 type III in myelination, this is not the sole NRG1 isoform expressed by DRG neurons. In particular DRG neurons express *NRG1 type I* [29], which is also processed by α–secretases [1] and its amino–acid sequence is identical to that of *NRG1 type III* in the region cleaved by *TACE*. Thus *TACE* could potentially affect myelination by inhibiting the processing of NRG1 type I. Similarly *TACE* could process other molecules regulating myelin formation.

To further investigate the role of *TACE* specific processing of NRG1 type III, we downregulated *TACE* activity in NRG1 type III null neurons (**Supplementary Fig. 8b**) and investigated whether ablation of *TACE* can rescue myelination in these neurons [1]. We infected *NRG1 type III*$^{-/-}$ DRG neurons with *TACE* specific shRNA (**Fig 8** sh1;

Supplementary Fig. 8a sh2 and sh3) or with a scrambled shRNA (shscr) control and rid the cultures of endogenous Schwann cells and fibroblasts. We then repopulated the neurons with rat primary Schwann cells and 21 days after induction of myelination, we examined MBP and neurofilament (**Fig. 8a**) expression by immunofluorescence and Western Blotting (**Supplementary Fig. 8c**) analyses. Ablation of *TACE* in *NRG1 type III*$^{-/-}$ neurons does not rescue myelination when *NRG1 type III* is absent (**Fig. 8**).

Since PI–3 Kinase is a key effector of NRG1 signaling and myelination, we have tested whether NRG1 cleaved by TACE or BACE1 modulates this pathway. Thus we incubated NRG1 β1 with either recombinant human TACE or BACE1 and determined p–AKT activation in starved primary rat Schwann cells. Importantly, NRG1 cleaved by TACE does not activate p–AKT (**Fig. 8c**), unlike BACE1 cleaved NRG1 (**Fig. 8d**). This result strongly suggests that TACE and BACE1 differentially activate NRG1 leading to either impairment (TACE) or activation (BACE1) of PI–3 Kinase signaling in Schwann cells and hence myelination. Furthermore, a lentiviral construct expressing *NRG1 type III* cDNA from the N-terminus until the histidine located between the identified TACE cleavage sites (**Fig. 7e**), unlike *full–length NRG1 type III*, rescues myelination of *NRG1 type III*$^{-/-}$ DRGs very inefficiently (**Fig. 8b**), despite being expressed on the axonal surface (**Fig. 8e**).

To further confirm the inhibitory role of TACE on NRG1 type III we tested whether *TACE*$^{+/-}$ animals, which myelinate normally, rescue hypomyelination of *NRG1 type III*$^{+/-}$ mice. Morphological analyses of compound *NRG1 type III*$^{+/-}$*//TACE*$^{+/-}$ P30 sciatic nerves (**Fig. 8f**) and *g* ratio measurements (**Fig 8g** and **Table 1**) showed that 50% reduction in TACE activity is sufficient to rescue myelination in *NRG1 type III*$^{+/-}$ animals.

Taken together, these results provide strong support that TACE inhibits myelination by modulating functional NRG1 type III levels on axonal membranes and describe a novel level of regulation of PNS myelination.

DISCUSSION

In this study we describe a novel inhibitory mechanism that regulates the extent of myelination in the PNS. As myelin is required for correct transmission of the electrical impulses along axons and for preservation of axonal integrity, understanding the processes directing myelin formation and assembly is important to develop effective treatments for demyelinating diseases. Using knockdown strategies and conditional inactivation of *TACE*, *in vitro* and *in vivo*, respectively, we show that this inhibitory role is neuron autonomous. We further demonstrate that TACE activity regulates NRG1 type III processing on axons and modulate PI–3 Kinase pathway in Schwann cells, thereby ensuring correct timing and myelination levels of PNS axons. These studies underscore the existence of several components controlling myelination and represent the first example of a negative control of myelination by secretases.

A number of secretases were previously implicated in regulating myelination. Among these only BACE1 [3, 5] and the zinc peptidase Nardylisin [30] have been directly linked to NRG1 type III cleavage; both positively regulate myelination. Biochemical studies have shown that BACE1 cleaves NRG1 type III [4]. As *BACE1*$^{-/-}$ mice are hypomyelinated in the CNS [5] and PNS [3], similar to *NRG1 type III*$^{+/-}$ mice [1, 2]; BACE1 cleavage of NRG1 type III is activating. Nardilysin was originally identified as an enhancer of the activity of ADAMs proteases, including TACE [30]. However, *Nardylisin*$^{-/-}$ mice are hypomyelinated in CNS and PNS rather than hypermyelinated as would be expected for a TACE hypomorph based on studies described here. These results suggest that Nardilysin may principally regulate other secretases that mediate NRG1 cleavage, including BACE1[30]. Moreover in this study, TACE mediates the cleavage of NRG1 type I [30], which we and others have shown is not involved in PNS myelination [1, 2].

A key finding is that these inhibitory effects of TACE directly oppose those of BACE1 [3-5], as indicated by differential activation of the PI–3 Kinase pathway in Schwann cells. *TACE* inactivation leads to an acceleration of the myelinating program *in vitro* and *in vivo*. Together these data indicate that secretases provide a post–transcriptional control of the amount of functional NRG1 type III and suggest that the balance between BACE1 and TACE activity is a key determinant of timing and extent of PNS myelination (**Supplementary Fig. 9**).

An important question is how the balance of NRG1 cleavage by these distinct secretases is regulated, including whether the cleavage by one secretase precludes processing by the others. The specificity achieved by sheddases, which normally process multiple substrates, has not been completely clarified. Several studies have reported that secretase do not recognize a specific amino-acid sequence [31]. This complexity is further enhanced by the fact that the same sheddase can process a single protein at different sites, as in the case of APP [32]. Thus, even if this is a highly conserved process, the actual mechanism through which regulated shedding occurs is unknown. Nonetheless, comparison of the amino–acid sequences of different substrates cleaved by the same secretase, together with the use of peptide libraries to identify putative consensus cleavage sequences, have helped in the identification of preferential amino acid used by secretases. Recent studies have reported that TACE selects small aliphatic residues immediately downstream of the cleavage site (P1' site). Of note, the isoleucine in P1' position of one of the cleavage sites we have identified by mass spectrometry, is among the preferred amino–acid for TACE cleavage [31].

TACE cleaves very close to the previously identified BACE1 cleavage site of NRG1 type III [4], suggesting that the two processing may be mutually exclusive. TACE and BACE1 frequently have common substrates although normally the corresponding cleavage sites are not nearby [33]. TACE and BACE1 processing of NRG1 type III most likely occurs at different subcellular locations, further strengthening the possibility that that these two events might be unique. TACE mature form is mainly located in the perinuclear space [34] and in the plasma membrane [35]. In addition both TACE and NRG1 colocalize in lipid rafts compartment, where they could interact [36, 37]. BACE1 instead is internalized from the plasma membrane to the endosomal compartments and then recycled to the late Golgi[33, 38]. As NRG1 molecules are glycosylated [39], they are most likely delivered to the plasma membrane via the trans Golgi network where they may be activated by BACE1. Whether BACE1 mediated cleavage of NRG1 type III also happens in endosomes and determine NRG1 type III recycling or degradation, as in the case of APP [40], is unknown. Further studies are required to establish the identity of the cellular organelles in which NRG1 type III processing occur, as the different localization could influence NRG1 type III mediated effects on myelination.

Our study suggests that *TACE* inhibits myelination by modulating NRG1 type III activity rather than total surface levels. Thus, in the absence of *TACE*, NRG1 active form is upregulated (**Fig. 7**). Our results indicate that TACE cleaves NRG1 type III in the β exon of the EGF domain, generating a non–functional molecule, which inefficiently rescue myelination of *NRG1 type III*$^{-/-}$ DRG neurons (**Fig. 8**). We suggest that these cleavages affect the affinity of NRG1 type III for the erbB2/3 heterodimer as indicated by increased erbB2/3–Fc binding in the absence of TACE (**Fig. 7**). In agreement, levels of p–Akt are increased in femoral nerves of *TACE*$^{-/-}$ mice (**Fig. 5**), and NRG1 cleaved by TACE does not activate PI–3 Kinase pathway in Schwann cells (**Fig. 8**). A corollary to these findings is that nearby cleavage by BACE1 enhances affinity for erbB receptors, as suggested by AKT phosphorylation (**Fig. 8**).

The effects of TACE cleavage are neuron autonomous. We have observed the hypermyelinating phenotype only when *TACE* is ablated in neurons further strengthening the likelihood that TACE acts on axonal NRG1 type III. More importantly, the hypermyelination closely resembles that of *NRG1 type III over-expressing mice* [2] and is due to an increase in the number of myelin lamellae. In addition, reduced TACE activity is sufficient to rescue myelination in *NRG1 type III*$^{+/-}$ mice. Further, ablation of neuronal *TACE* determines aberrant myelination of small caliber axons that would normally be unmyelinated, by probably altering the threshold levels of expression of axonal NRG1 type III [1]. Finally, inhibition of TACE in *NRG1 type III*$^{-/-}$ neurons is not enough to rescue the myelination defect of these neurons, further suggesting TACE processing of NRG1 type III. Nonetheless, we can not exclude that TACE might act on a separate molecule, which is not functional either because "inactive" or "absent" due to the absence of NRG1 type III. A likely candidate is the inhibitor of myelination Notch [17], although its processing is not altered. In agreement, it has been recently shown that ADAM 10 is the essential protease regulating Notch cleavage in a ligand dependent manner, whereas TACE participates in a ligand independent manner [41].

Surprisingly, defects in Remak bundles of *HB9Cre//TACE*$^{flx/flx}$ mice partially resembles that of *NRG1 type III*$^{+/-}$ mice [1]. Unlike these animals however, *HB9Cre//TACE*$^{flx/flx}$ mice are also characterized by unsorted fibers of large diameter, suggesting that in Remak bundles, TACE might cleave a different substrate. Of note *MAL*

overexpressing mice [42] have similar alterations and accumulation of $p75^{NTR}$, another target of TACE [6], in non-myelinating Schwann cells. Accordingly *TACE* inhibition alters the processing of $p75^{NTR}$. Although we can not exclude the contribution of $p75^{NTR}$, it has been suggested that glial and not axonal $p75^{NTR}$ promotes myelination in vitro[16] and remyelination in vivo[43]. That TACE might cleave molecules other than NRG1 type III, also implicated in myelination, is additionally suggested by the analysis of *P0Cre//TACE*$^{flx/flx}$ mice and by the reductions in the caliber of myelinated fibers in *HB9Cre//TACE*$^{flx/flx}$ mice.

In summary, we describe a novel mechanism controlling regulation of myelination during PNS development, via modulation of signaling pathway. Recent studies suggest that NRG1 type III may be dispensible for myelin maintenance, but important for remyelination [44,45]. Whether *TACE* plays a role during myelin maintenance or remyelination will require further investigations. The therapeutic potential of TACE modulation is underscored by the development of several compounds specifically targeting TACE and already tested in clinical trials for rheumatoid arthritis [46]. Thus, TACE inhibition may be a useful strategy to promote myelination in dysmyelinating peripheral neuropathies.

ACKNOWLEDGMENTS

This study was supported by Federazione Italiana Sclerosi Multipla (2007/PC/01) and Compagnia di San Paolo (C.T.), by National Institute of Health Grants, awards number R01-NS045630 (M.L.F.), R01-NS055256 (L.W.), R01-GM64750 (C.P.B.), RO1-NS26001 (J.L.S.) by Telethon Italia (GGP08021 to M.L.F., GGP071100 to L.W. and GPP10007 to C.T., L.W., M.L.F.). CT is a recipient of a FISM transition Career Award. We thank Drs Silvia Arber for providing the HB9 Cre transgenic line, Marie Filbin for antibodies, Paola Podini for assistance with electron microscopy, Giorgia Dina and Angela Cattaneo for excellent technical support and Yannick Poitelon for artwork.

AUTHOR CONTRIBUTIONS

R.L.-M conducted the majority of the experiments. F.C. and A.Q. performed morphological and ultrastructural analyses of sciatic nerves and ventral roots. K. H., C.P.B., M.L.F. and L.W provided transgenic lines and helped with inputs. A.B. performed the mass spectrometry analyses. J.L.S. provided support and initially contributed to the experimental design. C.T. designed the experimental plan, supervised the project and wrote the manuscript. All authors commented on the manuscript.

FIGURE LEGENDS

Figure 1. TACE downregulation induces precocious myelination and hypermyelination *in vitro*.

a) Western blotting analyses of rat Schwann cells uninfected or infected with lentiviruses expressing three different shRNA specific for *TACE* (*sh1, sh2* and *sh3*) or a scrambled artificial sequence (*shscr*). TACE and actin levels, as a loading control, were determined on a Li–Cor Odyssey 7 d after infection. TACE expression is significantly reduced in Schwann cells infected with *TACE* shRNAs, but not in scramble or uninfected samples.

b) Graph, average of three different experiments, showing approximately 80% reduction in TACE expression only in Schwann cells infected with *TACE* shRNAs. (**p = 0.0019 wt – sh1; **p = 0.0025 wt – sh2; ** p = 0.0018 wt – sh3). Error bars represent mean ± s.e.m.

c) Graph, average of three different experiments, showing quantitation of MBP+ segments 3 d after induction of myelination in control and infected cultures (*shTACE* and *shscr*). Quantitation was performed on the entire culture (total of 3 coverslips/ experiment; 3 different experiments). (**p = 0.0012 wt – sh1; **p = 0.0047 wt – sh2; *** p < 0.0001 wt – sh3). Error bars represent mean ± s.e.m.

d) Western blotting analyses of organotypic rat Schwann cells neuronal cocultures uninfected or infected with lentiviruses expressing *TACE* shRNA (*sh1, sh2* and *sh3*) or the scrambled artificial sequence (*shscr*). Lysates were tested for myelin protein zero (MPZ) and actin as a loading control, 14 d after induction of myelination. MPZ expression is significantly upregulated in TACE knocked down cultures.

e) Cocultures of organotypic rat Schwann cells neuronal cocultures infected with *TACE* specific shRNAs and scramble (*shscr*) lentiviruses were maintained in myelinating conditions for 3 d, fixed and stained for MBP (rhodamine) and neurofilament (fluorescein). Numerous myelin segments are evident in *shTACE*-infected cultures; none form in scramble-infected cultures and only few in uninfected cultures. Bar: 100 μm.

Figure 2. *In vitro* hypermyelination is neuronal cell autonomous.

a) Cocultures of murine neurons infected with *TACE sh1* shRNA or scramble shRNA (*shscr*), rid of endogenous Schwann cells and repopulated with *wild type* not infected rat Schwann cells were maintained in myelinating conditions for 14 d and then stained for MBP (rhodamine) and neurofilament (fluorescein). Numerous myelin segments are evident in *TACE sh1* infected cultures and fewer in uninfected and scramble infected cultures. Bar: 100 µm.

b) Graph, average of three different experiments showing quantitation of MBP+ segments 14 d after induction of myelination in control and neuronal infected cocultures (*shTACE* and *shscr*). Quantitation was performed on the entire culture (3 coverslips/ experiment; 3 different experiments). (***p = 0.0002 wt – sh1; ***p = 0.0007 wt – sh2; *** p = 0.0009 wt – sh3). Error bars represent mean ± s.e.m.

c) Cocultures of *wild type* uninfected mouse DRG neurons purified of endogenous Schwann cells and repopulated with rat Schwann cells previously infected with *TACE sh1* shRNA or scramble shRNA (*shscr*). Cultures were maintained in myelinating conditions for 21 d, and stained for MBP (rhodamine) and neurofilament (fluorescein). No difference in myelination is observed in infected versus control cultures. Bar: 100 µm.

d) Graph, average of three different experiments showing quantitation of MBP+ segments 21 d after induction of myelination in control and Schwann cells only infected cocultures (*shTACE* and *shscr*). Quantitation was performed on the entire culture (3 coverslips/ experiment; 3 different experiments). (p = not significant).

Figure 3. TACE inactivation in motor neurons leads to precocious myelination.

a) RT-PCR analyses showing high level of TACE mRNA expression in *wild type*, but not in *HB9Cre//TACE*$^{flx/flx}$ spinal cord mRNA. Schwann cells mRNA is used as positive control. GAPDH expression is a control for amplification.

b) Lysates of *wild type* and *HB9Cre//TACE*$^{flx/flx}$ P30 femoral nerves were fractionated by SDS PAGE and blotted with antibodies to TACE and actin as loading control. TACE expression is reduced in null femoral nerve extracts as compared to wild type extracts.

c) Electron micrographs of P1 ventral roots from *wild type* and HB9Cre//TACE$^{flx/flx}$ mice. In *HB9Cre//TACE*$^{flx/flx}$ fibers are hypermyelinated as compared to controls. Bar: 2µm.

d) Electron micrographs of P1 sciatic nerves from *wild type* and *HB9Cre//TACE*$^{flx/flx}$ mice; the majority of fibers in *HB9Cre//TACE*$^{flx/flx}$ mice are sorted and many already myelinated. Bar: 2µm.

Figure 4. *HB9Cre//TACE*$^{flx/flx}$ mice are hypermyelinated during development.

a) Semithin sections (top panels) and electron micrographs (bottom panels) of *wild type* and *HB9Cre//TACE*$^{flx/flx}$ P7 nerves. Bars: 15 µm (top panels) and 2 µm (bottom panels).

b) Semithin sections (top panels) and electron micrographs (bottom panels) of *wild type* and *HB9Cre//TACE*$^{flx/flx}$ P15 nerves. Bars: 20 µm (top panels) and 2 µm (bottom panels).

c) *g* ratio as a function of axon diameter are significantly different between *wild type* (red line) and *HB9Cre//TACE*$^{flx/flx}$ P7 mice (black line) mice ($p = 0.0007$). The graph represent the *g* ratio obtained from more than myelinated 500 axons (total of 3 animals per genotype).

d) Distribution of myelinated fibers is similar in *HB9Cre//TACE*$^{flx/flx}$ and *wild type* P7 sciatic nerves (p = not significant). Over 500 fibers for each genotype (n=3) were counted.

e) High power images of myelinated axons of similar diameters demonstrate that myelin in *wild type* vs *HB9Cre//TACE*$^{flx/flx}$ sciatic nerves have identical periodicity but significantly differ in the number of lamellae. Bar: 500 nm.

Figure 5. *HB9Cre//TACE*$^{flx/flx}$ adult mice are hypermyelinated and Remak fibers are aberrantly ensheathed.

a) Semithin sections (top panels) and electron micrographs (bottom panels) of *wild type* and *HB9Cre//TACE*$^{flx/flx}$ P30 ventral roots. Bars: 20 µm (top panels) and 2 µm (bottom panels). Asterisks indicate heavily myelinated fibers of less than 1 µm in diameter.

b) Semithin sections (top panels) and electron micrographs (bottom panels) of *wild type* and *HB9Cre//TACE*$^{flx/flx}$ P30 sciatic nerves. Bars: 20 µm (top panels) and 2 µm (bottom panels).

c) Lysates of *wild type* and *HB9Cre//TACE*$^{flx/flx}$ P15 and P30 femoral nerves were blotted with antibodies to MBP and actin as loading control. MBP expression is upregulated in femoral nerve extracts from TACE null mice.

d) Lysates of *wild type* and *HB9Cre//TACE*$^{flx/flx}$ P30 femoral nerves were blotted with antibodies to p–AKT (ser 473), total AKT and actin as loading control. p–AKT expression is significantly upregulated in null femoral nerve extracts.

e) Impaired sorting of Remak fibers of *HB9Cre//TACE*$^{flx/flx}$ sciatic nerves. In *wild type* mice unmyelinated axons are segregated into separate pockets of Remak bundles and fully wrapped by Schwann cells. In *HB9Cre//TACE*$^{flx/flx}$ mice Remak bundles contain abnormally large caliber axons (asterisks) and Schwann cells fail to ensheath the axons. Bar: 1 μm.

f) *g* ratio as a function of axon diameter are significantly different between *wild type* (red line) and *HB9Cre//TACE*$^{flx/flx}$ P30 sciatic nerve fibers (black line) mice ($p < 0.0001$). The graph represent the *g* ratio obtained from more than 700 myelinated axons (3 animals per genotype).

g) Myelinated axons in *HB9Cre//TACE*$^{flx/flx}$ P30 sciatic nerves are significantly smaller (***$p < 0.0001$ **$p = 0.0051$). Approximately 7% of myelinated fibers are less than 1 μm in diameter in TACE null sciatic nerves. Over 1700 axons for each genotype (n=3) were counted. Error bars represent mean ± s.e.m.

Figure 6. *P0Cre//TACE*$^{flx/flx}$ mice are normally myelinated.

a) Genotyping PCR on genomic DNA prepared from sciatic nerves of P15 *wild type* and *P0Cre//TACE*$^{flx/flx}$ animals. The null allele is present only in *floxed TACE* nerves expressing the Cre allele.

b) *P0Cre//TACE*$^{flx/flx}$ have comparable myelin thickness. Semithin sections (top panels) and electron micrographs (bottom panels) of *wild type* and *P0Cre//TACE*$^{flx/flx}$ P7 sciatic nerves. Bars: 20 μm (top panels) and 2 μm (bottom panels).

c) *P0Cre//TACE*$^{flx/flx}$ have comparable myelin thickness. Semithin sections (top panels) and electron micrographs (bottom panels) of *wild type* and *P0Cre//TACE*$^{flx/flx}$ P30 sciatic nerves. Bars: 20 μm (top panels) and 2 μm (bottom panels).

d) Lysates of wild type and *P0Cre//TACE*$^{flx/flx}$ P15 sciatic nerves were fractionated by SDS PAGE and blotted with antibodies to myelin proteins (MAG and MBP) and actin as loading control. No alteration in myelin protein expression is observed among *wild type* and *null* animals.

e) *g* ratio as a function of axon diameter are identical in *wild type* (red line) and *P0Cre//TACE*$^{flx/flx}$ P30 sciatic nerve fibers (black line) mice (p = not significant). The graph represent the *g* ratio obtained from more than 300 myelinated axons (3 animals per genotype).

f) *P0Cre/TACE*$^{flx/flx}$ mice have a slight but significant increase in their axonal diameters as compared to *wild type* (***p < 0.0001, ** p<0.001). Myelinated axons of P30 sciatic nerves were binned based on their axonal diameters. More than 1200 axons were counted from 3 different animals per genotype. Error bars represent mean ± s.e.m.

Figure 7. TACE cleaves NRG1 type III

a) Lysates of *wild type*, *TACE*$^{+/-}$ and *TACE*$^{-/-}$ DRG neurons were blotted with an antibody to NRG1 (sc–348) and actin as loading control. The 135 kD band corresponding to full length NRG1 pro–protein (arrowhead) is increased in *TACE*$^{+/-}$ and even more in *TACE*$^{-/-}$ lysates. The active cleaved fragment of NRG1 (arrow) is upregulated *TACE*$^{+/-}$ and in *TACE*$^{-/-}$ samples.

b) Lysates of *wild type* and *HB9Cre//TACE*$^{flx/flx}$ P30 femoral nerves were blotted with antibodies to NRG1 and actin as loading control. NRG1 uncleaved product is present in *wild type* but not in *TACE*$^{-/-}$ nerves (arrowhead), contrary to the cleaved, active NRG1 fragment, which is upregulated in null samples (arrow).

c) In vitro cleavage of human recombinant NRG1 β1 EGF domain. NRG1 β1 was incubated with human recombinant TACE and then separated on a SDS page gel. The corresponding cleaved band (arrow) was digested with trypsin and analyzed by MALDI–TOF mass spectrometry.

d) MALDI–TOF spectrum of the 6.5 KDa band digested with endoproteinase Glu–C. Peaks with arrows are from NRG1, unlabeled peaks are from autolysis of endoproteinase Glu-C.

e) NRG1 β 1 sequence representing the EGF domain (red), the β1 exon (yellow box) and the transmembrane domain (blue). TACE (α) and BACE1 (β) cleavage sites are also indicated.

f) Cultures of *wild type* and *TACE*$^{-/-}$ DRG neurons were incubated with erbB2/3-Fc and the binding visualized with rhodamine-conjugated anti-human Fc antibodies (rhodamine); neurofilament staining from corresponding fields is shown (fluorescein). Bar: 50 μm.

g) Graph, average of three different experiments, showing quantitation of erbB2/B3 binding signal. Quantitation was performed on confocal images acquired with the same z-stack and laser intensity, using Image J software analyses (total of 5 coverslips/ experiment; 3 different experiments). (***$p < 0.0001$). Error bars represent mean ± s.e.m.

Figure 8. TACE regulates NRG1 type III activity.

a) Cocultures of *wild type* and *NRG1 type III*$^{-/-}$ DRG neurons uninfected or infected with *TACE sh1* shRNA or scramble shRNA (*shscr*) were maintained in myelinating conditions with rat Schwann cells for 21 d and then stained for MBP (rhodamine) and neurofilament (fluorescein). TACE knock down does not rescue myelination in *NRG1 type III*$^{-/-}$ neurons. Bar: 50 µm.

b) Cocultures of *wild type* or *NRG1 type III*$^{-/-}$ DRG neurons uninfected or infected with *full length NRG1 type III* or *NRG1 cleaved at the TACE cleavage site*, were maintained in myelinating conditions with *wild type* rat Schwann cells for 14 d; fixed and stained for MBP (rhodamine) and neurofilament (fluorescein). NRG1 cleaved by TACE inefficiently rescue does myelination in *NRG1 type III*$^{-/-}$ neurons. Shown are the few MBP+ segments observed (9 coverslips/3 experiments) Bar: 50 µm.

c) Lysates of rat primary Schwann cells starved for 16 h, not stimulated (control) or stimulated with 50 ng/ml NRG1 β1 (NRG1), 50 ng/ml NRG1 β1 cleaved by TACE (NRG1+TACE) or by 50 ng/ml TACE alone (TACE), were blotted with antibodies to p–AKT (ser 473), total AKT and calnexin as loading control.

d) Lysates of rat primary Schwann cells starved for 16 hrs, not stimulated (control) or stimulated with 50 ng/ml NRG1 β1 (NRG1), 50 ng/ml NRG1 β1 cleaved by BACE1 (NRG1+BACE1) or by 50 ng/ml BACE1 alone (BACE1), were blotted with antibodies to p–AKT (ser 473), total AKT and calnexin as loading control.

e) NRG1 cleaved by TACE is detected on the axonal surface of *NRG1 type III*$^{-/-}$ infected neurons. Live staining for the NRG1 HA epitope (rhodamine) and neurofilament (fluorescein). Bar: 50 µm.

f) Electron micrographs of *NRG1 type III*$^{+/-}$, compound *NRG1 type III*$^{+/-}$//*TACE*$^{+/-}$, and *wild type* P30 sciatic nerves. *NRG1 type III*$^{+/-}$//*TACE*$^{+/-}$ fibers are normally myelinated. Bar: 2 µm.

g) *g* ratio as a function of axon diameter is reduced in compound *NRG1 type III*$^{+/-}$ //*TACE*$^{+/-}$ mice (black line) as compared to *NRG1 type III*$^{+/-}$ P30 sciatic nerve fibers (red line) ($p < 0.0001$). The graph represent the *g* ratio obtained from more than 200 myelinated axons (3 animals per genotype).

MATERIALS AND METHODS

Mice and genotyping

Generation of *TACE floxed* mice has been previously reported [21]. Mice were genotyped by PCR using the following primers: 5' TTACTCTTCTTACTAACAGTCCCCTG 3' and 5' AACTATCTCAAACAATAAGCTGAAGTG 3'. *Homozygous TACE floxed* animals were crossed with *HB9-Cre transgenic* line to specifically delete TACE in motor neurons, with *mP0TOT-cre* transgenic line to ablate TACE in Schwann cells and with *CMV-Cre* transgenic line to generate complete null animals. Generation of the *HB9-Cre, P0-Cre, CMV-Cre* transgenic lines have been previously described[22, 27, 28]. The genotype was performed by PCR analyses on genomic DNA. PCR was carried out at 94°C for 30 sec, 60°C for 30 s and 72°C for 30 s, followed by 5 min extension at 72°C for 40 cycles. The expected 850 nt product for wild type allele and 1000 nt product for the floxed allele were separated on a 1% agarose gel. The presence of the null allele was also determined by PCR on genomic DNA using the following primers: 5' TTACTCTTCTTACTAACAGTCCCCTG 3' and 5' GGGAGAGCCACACCTTGACC 3'. PCR was carried at 94°C for 30 s, 60°C for 30 s and 72°C for 30 s, followed by 5 min extension at 72°C for 40 cycles. The amplified fragment of 400 nt, corresponding to the null allele, was analyzed on a 1% agarose gel. Generation and analyses of *NRG1 type III*$^{-/-}$ and *NRG1 type III*$^{+/-}$ animals have been previously described [1].

All experiments involving animals followed protocols approved by the Animal care and Use Committee of San Raffaele Scientific Institute.

Cell cultures

Mouse DRG neurons were isolated from E14.5 embryos and established on collagen-coated glass coverslips as described [1]. Explants were cycled with FUDR to eliminate all non-neuronal cells. Neuronal media was supplemented with 50 ng/ml NGF (Harlan, Bioproducts for Science). Primary rat Schwann cells were prepared as described [1] and maintained in DMEM (BioWhittaker), 10% FBS (Invitrogen), 2 mM L-glutamine (Invitrogen), until used. Rat Schwann cells were added (200,000 cells/coverslip) to

establish explant cultures of DRG neurons and myelination was initiated by supplementing media with 50 µg/ml ascorbic acid (Sigma-Aldrich).

Fc fusion proteins and binding experiments

Established explants of *TACE*$^{-/-}$, *wild type*, and DRG neurons previously infected with shRNA against *TACE* were incubated with supernatant containing erbB2/erbB3-Fc and an anti-human Fc (Jackson Immunoresearch) as described [1]. Quantitation was performed on confocal images from three different experiments (5 coverslips/experiment). All images with the same magnification, z-stack and laser intensity were analyzed using Image J version 1.44.

Lentiviral production and infection

Individual shRNAs clones (TRCN0000031949, TRCN0000031952 and TRCN0000031953) specifically targeting mouse *TACE* were obtained through the RNAi Consortium (Open Biosystem). Lentiviral vectors were transfected into 293FT cells (Invitrogen) together with packaging plasmids pLP1, pLP2 and pLP/VSVG plasmids (Invitrogen) using Lipofectamine 2000 (Invitrogen) according to manufacturer's instructions. As control, we used a vector encoding an shRNA directed against a nonspecific oligonucleotide: 5'-TCGTACGCGCAATACTTCGA-3' whose sequence had been verified by BLAST search against the human and the mouse genome. The scramble shRNA lentiviral vector was cloned in the pLL3.7 and produced as described [47]. Full length *NRG1 type III* lentivirus was generated as described[1]. The cDNA encoding *NRG1 type III* from the N terminus until the histidine between the identified TACE cleavage sites was amplified by PCR with the following primers: 5' CAGATCACTAGTATGGAGATTTATTCCCCAGAC 3' and 5'CACTTTCTCGA GTTAATGTTTGTAGAAGCTGGC 3', using as template full length NRG1 type III HA tagged in the extracellular region, cloned in a pLenti6/V5 plasmid with standard molecular biology techniques and confirmed by sequencing.

Viral supernatants were collected 48 h after transfection, centrifuged at 3,000 rpm for 15 min, aliquoted for one-time use, and frozen at –80°C. Freshly plated Schwann cells (10^6 cells per 100–mm plate) were incubated for 2 d with viruses at a 2/3 dilution (vol/vol) in

DMEM, 10% FBS, and 2 mM L-glutamine supplemented with forskolin and rh NRG-1 (EGF domain, R&D). Cells were expanded for an additional week and maintained for 3 d in Schwann cell media before use. Protein knockdowns were confirmed by Western blotting. Mouse DRG neuronal explants were infected the day after the dissection and left in the presence of the virus for 24 h after which cultures were purified of endogenous Schwann cell to obtain pure DRG neurons by cycling them with antimitotic reagents or cultured with endogenous Schwann cell. In the latter case both DRG neurons and mouse primary Schwann cell were infected.

Electron microscopy and morphological analyses

Semithin and ultrathin sections were obtained as previously described [48]. Tissues were removed and fixed with 2% glutaraldehyde in 0.12 M phosphate buffer, postfixed with 1% osmium tetroxide, and embedded in Epon (Fluka). Semithin sections (0.5–1 μm thick) were stained with toluidine blue and examined by light microscopy (Olympus BX51). Ultrathin sections (100–120 nm thick) were stained with uranile acetate and lead citrate and examined by electron microscopy (Leo 912 Omega). Digitized non overlapping semithin sections images from corresponding levels of the sciatic nerve were obtained with a digital camera (Leica DFC300F) using a 100 x objective. *g*-ratio measurements were performed on digitized non overlapping electron micrographs images. *g*-ratio was determined by dividing the mean diameter of an axon without myelin by the mean diameter of the same axon with myelin. More than a 300 randomly chosen fibers per animal were analyzed for P30 *g*–ratio measurements and more than 200 for *g*–ratio measurements at P7.

To determine the size distribution of myelinated fibers in sciatic nerves, diameters of all fibers in at least 10 images of randomly chosen representative images were measured and binned based on their width. All measurements were acquired on a 100 x semithin sections images using a Image J software.

TACE and BACE1 Cleavage reaction

1 μg of human recombinant TACE (R&D Development cat # 930ADB) was incubated with 2 μg of human recombinant NRG1 β1 that differs from the mouse sequence by one

amino-acid upstream of the EGF domain (R&D Development cat # 396-HB, residues 176-246), for 16 h at 37°C in the presence of $ZnCl_2$ and then separated on a Tris-Tricine gel together with native uncleaved NRG1 β1 protein for comparison. The gel was stained with Comassie Blue and then processed for mass spectrometry analysis.

To test TACE and BACE1 cleavage effects of NRG1 signaling, 1 or 2 μg of human recombinant TACE or BACE1 (R&D Development cat # 931-AS) were incubated with 0.5 μg of human recombinant NRG1 β1 for 16 h at 37°C. Cleaved NRG1 β1 was used to stimulate serum starved, rat primary Schwann cells for 20 min at 37°C. Cells were then lysed and analyzed by Western Blotting for PI3–K intermediate pathways.

MALDI-TOF MS analysis

Band of interest was excised from gels, subjected to reduction by 10 mM DTT and alkylation by 55 mM iodoacetamide, and finally digested overnight with Endoproteinase Glu-C (Roche). 10 μl of supernatant mixture from digestion were acidified with formic acid up to a final concentration of 10%, desalted with StageTipμC18 (Proxeon Biosystem, Denmark) [49] and analyzed on a MALDI-TOF Voyager-DE STR (Applied Biosystems) mass spectrometer using the dried droplet technique and alpha-cyano-4-hydroxycinnamic acid as matrix. Spectra were acquired in reflector positive ion mode, accumulated over a mass range of 750–4000 Da with a mean resolution of about 15000; then internally calibrated using matrix signals and Glu-C autolysis peaks and processed *via* Data Explorer software version 4.0.0.0 (Applied Biosystems). Assignment of MH+ peaks was manually done using GPMAW software (version 8.10).

RNA isolation and measurements

Total RNA was isolated from purified rat Schwann cells, mouse purified DRG neurons, and spinal cord using Trizol (Roche), according to manufacturer's instruction. Total RNA was retro-transcribed to cDNA as previously described [50]. Aliquots of RT products were tested in parallel using primers pair for TACE (5'-TTGAAGAATACTTGTAAATT-3' and 5'-GGGTTGTAATAAGCTTTTGG-3'; 94°C for 30 s, 52°C for 30 s and 72°C for 60 s, followed by 5 min extension at 72°C for 30 cycles).

Preparation of detergent lysates and immunoblotting

Tissues and cell cultures were Dounce homogenized in a lysis buffer containing 2% SDS, 95 mM NaCl, 10 mM EDTA, anti-phosphatases inhibitor (PhoSTOP Roche) and anti-protease inhibitors (Complete-Mini EDTA free Roche). Homogenates were boiled 5 min, centrifuged 10 min at 14,000 rpm at 16°C. Supernatants were aliquoted and stored at –80°C until used. Protein concentrations were determined by the BCA method (Pierce); samples (20-40 µg of protein) were fractionated by SDS-PAGE and blotted onto nitrocellulose (Protran Biosciences). Membranes were blocked in 5% BSA, 0.05% sodium azide in TBST (0.1% TritonX-100 in TBS). Appropriate regions were excised, incubated with specific primary and secondary antibodies, washed in TBST and developed with the SuperSignal chemiluminescent substrate (Pierce). For quantitative Western Blotting analyses, filters were analyzed using the Odyssey Infrared Imaging System (LI-COR Biosciences) according to manufacturer's instructions.

Antibodies and immunofluorescence

Mouse monoclonal antibodies included anti–MBP (SMI–94, SMI–99), neurofilament (SMI–31 and SMI–32) (Sternberger Monoclonals) and Notch–1 (NICD) (Chemicon). Rabbit polyclonal antibodies included anti–NRG sc348 (Santa Cruz), MAG, MPZ (M. Filbin, Hunter College, New York, NY), actin (Sigma–Aldrich), peripherin, TACE and $p75^{NTR}$ (Chemicon), phospho–AKT (ser 473) and total AKT (Cell Signaling). Chicken antibodies include anti–neurofilament M (Covance). Secondary antibodies conjugated to rhodamine, fluorescein, coumarin, Cy5, or HRP were obtained from Jackson Immunoresearch. Infrared secondary antibodies for quantitative Western blotting analyses (Goat anti–Rabbit and Goat anti–Mouse IRDye 680 or IRDye 800) were obtained from LI–COR Biosciences. Cocultures were fixed in 4% paraformaldheyde and permeabilized in 100 % methanol at –20°C for 15 min, stained as described [1] and examined by epifluorescence on a Nikon E800 microscope and by confocal microscopy on a Zeiss LSM 510 or on a Leica SP5.

Statistical analysis

Statistical analyses (Fischers' s exact test, Chi square, and t-test) were performed using the Prism Software package (GraphPad).

REFERENCES

1. Taveggia, C. et al. Neuregulin-1 type III determines the ensheathment fate of axons. *Neuron* **47**, 681-94 (2005).
2. Michailov, G.V. et al. Axonal neuregulin-1 regulates myelin sheath thickness. *Science* **304**, 700-3 (2004).
3. Willem, M. et al. Control of peripheral nerve myelination by the beta-secretase BACE1. *Science* **314**, 664-6 (2006).
4. Hu, X. et al. Genetic deletion of BACE1 in mice affects remyelination of sciatic nerves. *Faseb J* **22**, 2970-80 (2008).
5. Hu, X. et al. Bace1 modulates myelination in the central and peripheral nervous system. *Nat Neurosci* **9**, 1520-5 (2006).
6. Yang, P., Baker, K.A. & Hagg, T. The ADAMs family: coordinators of nervous system development, plasticity and repair. *Prog Neurobiol* **79**, 73-94 (2006).
7. Shirakabe, K., Wakatsuki, S., Kurisaki, T. & Fujisawa-Sehara, A. Roles of Meltrin beta /ADAM19 in the processing of neuregulin. *J Biol Chem* **276**, 9352-8 (2001).
8. Yokozeki, T. et al. Meltrin beta (ADAM19) mediates ectodomain shedding of Neuregulin beta1 in the Golgi apparatus: fluorescence correlation spectroscopic observation of the dynamics of ectodomain shedding in living cells. *Genes Cells* **12**, 329-43 (2007).
9. Wakatsuki, S., Yumoto, N., Komatsu, K., Araki, T. & Sehara-Fujisawa, A. Roles of meltrin-beta/ADAM19 in progression of Schwann cell differentiation and myelination during sciatic nerve regeneration. *J Biol Chem* **284**, 2957-66 (2009).
10. Sagane, K. et al. Ataxia and peripheral nerve hypomyelination in ADAM22-deficient mice. *BMC Neurosci* **6**, 33 (2005).
11. Ozkaynak, E. et al. Adam22 is a major neuronal receptor for Lgi4-mediated Schwann cell signaling. *J Neurosci* **30**, 3857-64 (2010).
12. Freese, C., Garratt, A.N., Fahrenholz, F. & Endres, K. The effects of alpha-secretase ADAM10 on the proteolysis of neuregulin-1. *Febs J* **276**, 1568-80 (2009).
13. Horiuchi, K., Zhou, H.M., Kelly, K., Manova, K. & Blobel, C.P. Evaluation of the contributions of ADAMs 9, 12, 15, 17, and 19 to heart development and ectodomain shedding of neuregulins beta1 and beta2. *Dev Biol* **283**, 459-71 (2005).
14. Blobel, C.P. ADAMs: key components in EGFR signalling and development. *Nat Rev Mol Cell Biol* **6**, 32-43 (2005).
15. Peschon, J.J. et al. An essential role for ectodomain shedding in mammalian development. *Science* **282**, 1281-4 (1998).
16. Cosgaya, J.M., Chan, J.R. & Shooter, E.M. The neurotrophin receptor p75NTR as a positive modulator of myelination. *Science* **298**, 1245-8 (2002).
17. Woodhoo, A. et al. Notch controls embryonic Schwann cell differentiation, postnatal myelination and adult plasticity. *Nat Neurosci* **12**, 839-47 (2009).
18. Zampieri, N., Xu, C.F., Neubert, T.A. & Chao, M.V. Cleavage of p75 neurotrophin receptor by alpha-secretase and gamma-secretase requires specific receptor domains. *J Biol Chem* **280**, 14563-71 (2005).
19. van Tetering, G. et al. Metalloprotease ADAM10 is required for Notch1 site 2 cleavage. *J Biol Chem* **284**, 31018-27 (2009).
20. Weber, S. et al. The disintegrin/metalloproteinase Adam10 is essential for epidermal integrity and Notch-mediated signaling. *Development* **138**, 495-505 (2011).

21. Horiuchi, K. et al. Cutting edge: TNF-alpha-converting enzyme (TACE/ADAM17) inactivation in mouse myeloid cells prevents lethality from endotoxin shock. *J Immunol* **179**, 2686-9 (2007).
22. Yang, X. et al. Patterning of muscle acetylcholine receptor gene expression in the absence of motor innervation. *Neuron* **30**, 399-410 (2001).
23. Donald, D. A relation between axone diameter and myelination determined by measurement of myelinated spinal root fibers. *Journal of Comparative Neurology* **60**, 437-471 (1934).
24. Windebank, A.J., Wood, P., Bunge, R.P. & Dyck, P.J. Myelination determines the caliber of dorsal root ganglion neurons in culture. *J Neurosci* **5**, 1563-9 (1985).
25. Maurel, P. & Salzer, J.L. Axonal regulation of Schwann cell proliferation and survival and the initial events of myelination requires PI 3-kinase activity. *J Neurosci* **20**, 4635-45 (2000).
26. Ogata, T. et al. Opposing extracellular signal-regulated kinase and Akt pathways control Schwann cell myelination. *J Neurosci* **24**, 6724-32 (2004).
27. Schwenk, F., Baron, U. & Rajewsky, K. A cre-transgenic mouse strain for the ubiquitous deletion of loxP-flanked gene segments including deletion in germ cells. *Nucleic Acids Res* **23**, 5080-1 (1995).
28. Feltri, M.L. et al. Conditional disruption of beta 1 integrin in Schwann cells impedes interactions with axons. *J Cell Biol* **156**, 199-209 (2002).
29. Meyer, D. et al. Isoform-specific expression and function of neuregulin. *Development* **124**, 3575-86 (1997).
30. Ohno, M. et al. Nardilysin regulates axonal maturation and myelination in the central and peripheral nervous system. *Nat Neurosci* **12**, 1506-13 (2009).
31. Caescu, C.I., Jeschke, G.R. & Turk, B.E. Active-site determinants of substrate recognition by the metalloproteinases TACE and ADAM10. *Biochem J* **424**, 79-88 (2009).
32. Yang, H.C. et al. Biochemical and kinetic characterization of BACE1: investigation into the putative species-specificity for beta- and beta'-cleavage sites by human and murine BACE1. *J Neurochem* **91**, 1249-59 (2004).
33. Thinakaran, G. & Koo, E.H. Amyloid precursor protein trafficking, processing, and function. *J Biol Chem* **283**, 29615-9 (2008).
34. Schlondorff, J., Becherer, J.D. & Blobel, C.P. Intracellular maturation and localization of the tumour necrosis factor alpha convertase (TACE). *Biochem J* **347 Pt 1**, 131-8 (2000).
35. Doedens, J.R. & Black, R.A. Stimulation-induced down-regulation of tumor necrosis factor-alpha converting enzyme. *J Biol Chem* **275**, 14598-607 (2000).
36. Tellier, E. et al. The shedding activity of ADAM17 is sequestered in lipid rafts. *Exp Cell Res* **312**, 3969-80 (2006).
37. Frenzel, K.E. & Falls, D.L. Neuregulin-1 proteins in rat brain and transfected cells are localized to lipid rafts. *J Neurochem* **77**, 1-12 (2001).
38. Koo, E.H. & Squazzo, S.L. Evidence that production and release of amyloid beta-protein involves the endocytic pathway. *J Biol Chem* **269**, 17386-9 (1994).
39. Burgess, T.L., Ross, S.L., Qian, Y.X., Brankow, D. & Hu, S. Biosynthetic processing of neu differentiation factor. Glycosylation trafficking, and regulated cleavage from the cell surface. *J Biol Chem* **270**, 19188-96 (1995).
40. Haass, C., Koo, E.H., Mellon, A., Hung, A.Y. & Selkoe, D.J. Targeting of cell-surface beta-amyloid precursor protein to lysosomes: alternative processing into amyloid-bearing fragments. *Nature* **357**, 500-3 (1992).
41. Bozkulak, E.C. & Weinmaster, G. Selective use of ADAM10 and ADAM17 in activation of Notch1 signaling. *Mol Cell Biol* **29**, 5679-95 (2009).

42. Buser, A.M. et al. The myelin protein MAL affects peripheral nerve myelination: a new player influencing p75 neurotrophin receptor expression. *Eur J Neurosci* **29**, 2276-90 (2009).
43. Tomita, K. et al. The neurotrophin receptor p75NTR in Schwann cells is implicated in remyelination and motor recovery after peripheral nerve injury. *Glia* **55**, 1199-208 (2007).
44. Fricker, F.R. et al. Sensory axon-derived neuregulin-1 is required for axoglial signaling and normal sensory function but not for long-term axon maintenance. *J Neurosci* **29**, 7667-78 (2009).
45. Fricker, F.R. et al. Axonally derived neuregulin-1 is required for remyelination and regeneration after nerve injury in adulthood. *J Neurosci* **31**, 3225-33 (2011).
46. Moss, M.L., Sklair-Tavron, L. & Nudelman, R. Drug insight: tumor necrosis factor-converting enzyme as a pharmaceutical target for rheumatoid arthritis. *Nat Clin Pract Rheumatol* **4**, 300-9 (2008).
47. Maurel, P. et al. Nectin-like proteins mediate axon Schwann cell interactions along the internode and are essential for myelination. *J Cell Biol* **178**, 861-74 (2007).
48. Quattrini, A. et al. Beta 4 integrin and other Schwann cell markers in axonal neuropathy. *Glia* **17**, 294-306 (1996).
49. Shevchenko, A., Wilm, M., Vorm, O. & Mann, M. Mass spectrometric sequencing of proteins silver-stained polyacrylamide gels. *Anal Chem* **68**, 850-8 (1996).
50. Wrabetz, L. et al. A minimal human MBP promoter-lacZ transgene is appropriately regulated in developing brain and after optic enucleation, but not in shiverer mutant mice. *J Neurobiol* **34**, 10-26 (1998).

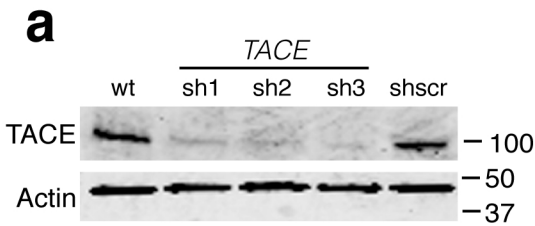
a
TACE
wt
sh1
sh2
sh3
shscr
TACE
Actin
100
50
37

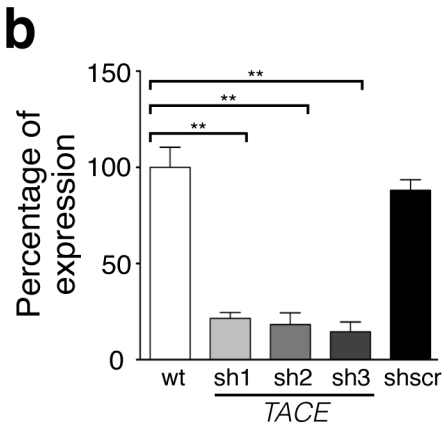
b
Percentage of expression
150
100
50
0
**
**
**
wt
sh1
sh2
sh3
shscr
TACE

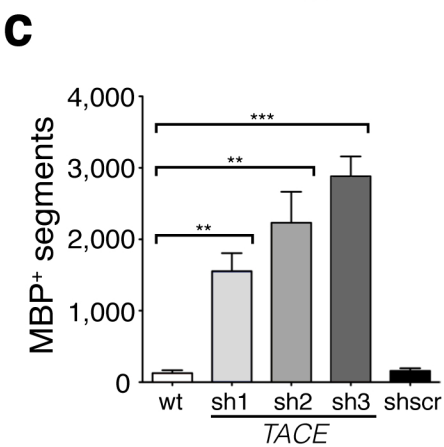
c
MBP+ segments
4,000
3,000
2,000
1,000
0
***
**
**
wt
sh1
sh2
sh3
shscr
TACE

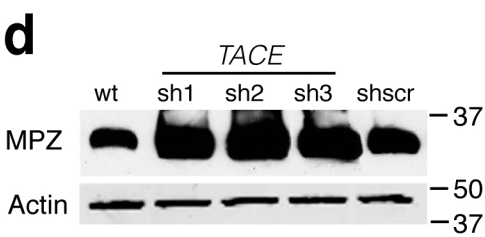
d
TACE
wt
sh1
sh2
sh3
shscr
MPZ
Actin
37
50
37

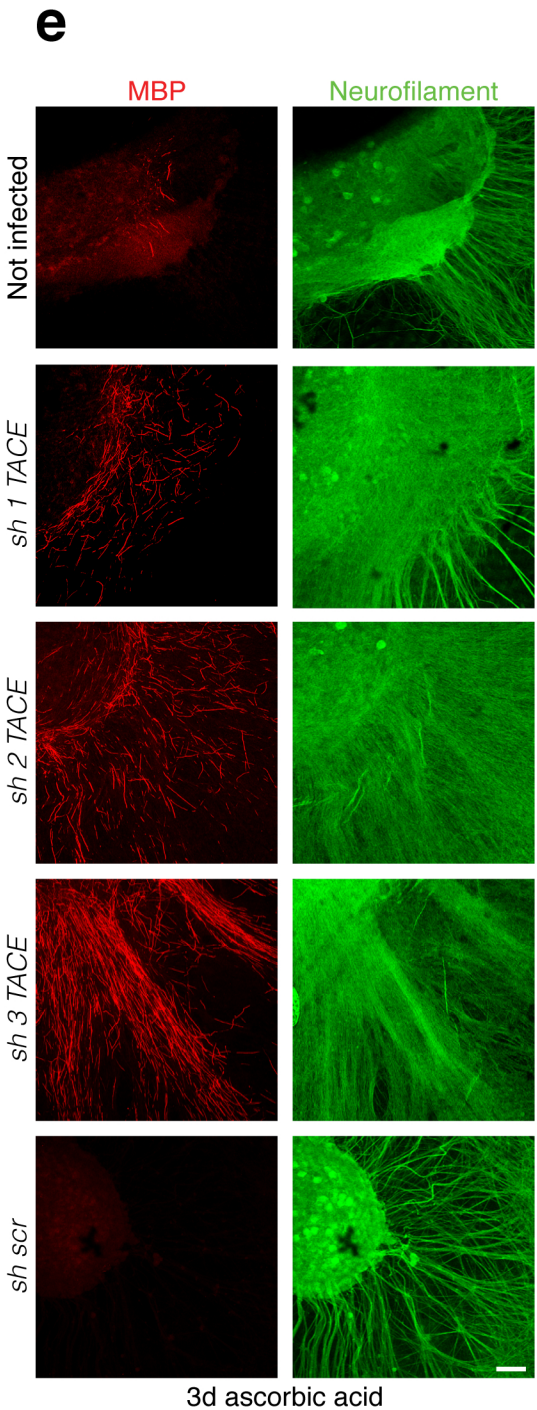
e
MBP
Neurofilament
Not infected
sh 1 TACE
sh 2 TACE
sh 3 TACE
sh scr
3d ascorbic acid

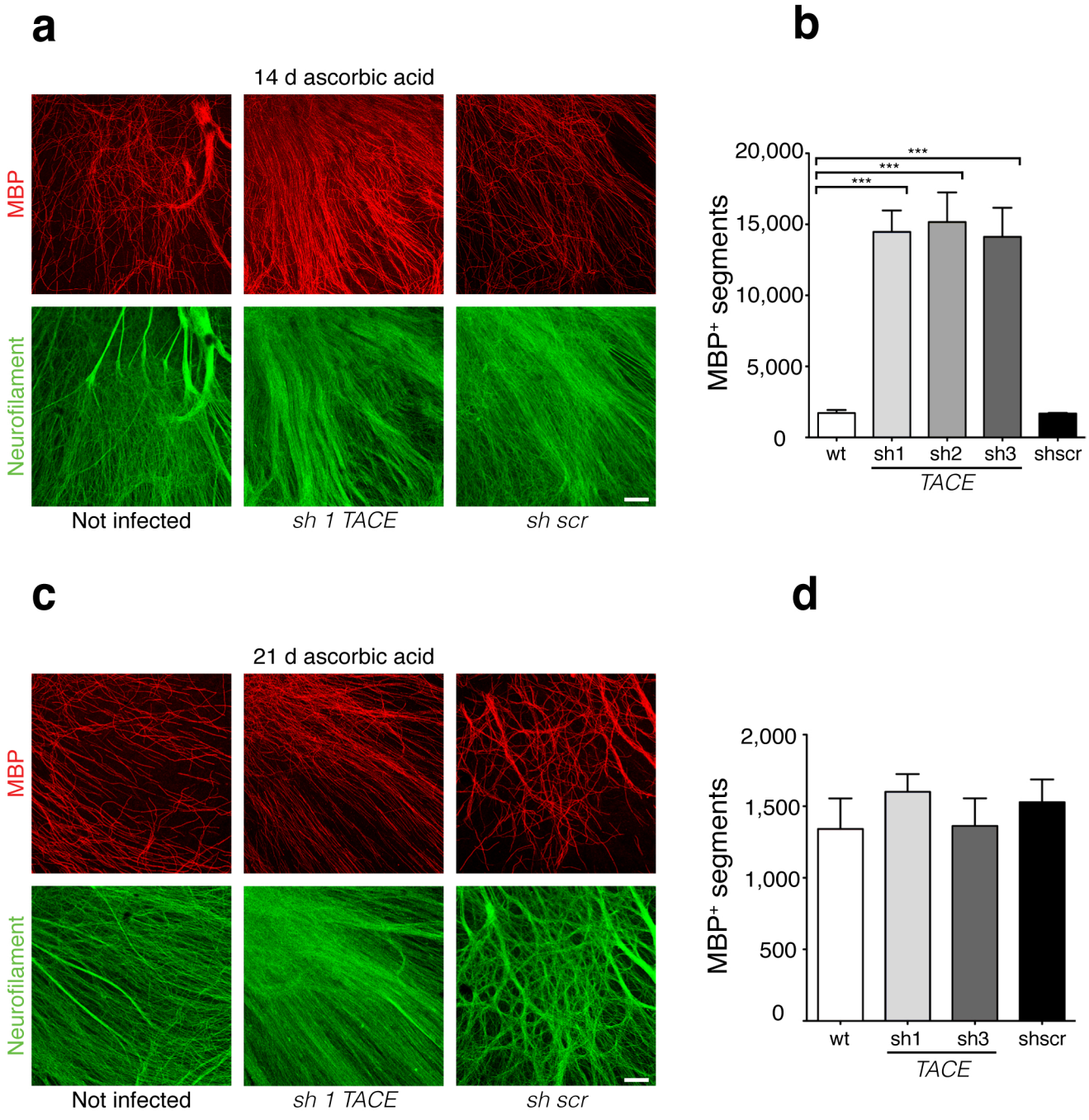
a
14 d ascorbic acid
MBP
Neurofilament
Not infected
sh 1 TACE
sh scr
b
MBP+ segments
20,000
15,000
10,000
5,000
0
***
***
***
wt
sh1
sh2
sh3
shscr
TACE
c
21 d ascorbic acid
MBP
Neurofilament
Not infected
sh 1 TACE
sh scr
d
MBP+ segments
2,000
1,500
1,000
500
0
wt
sh1
sh3
shscr
TACE

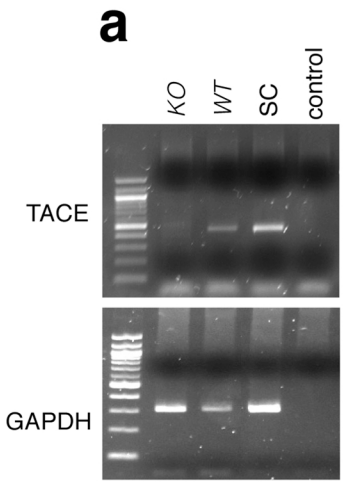
a
KO
WT
SC
control
TACE
GAPDH

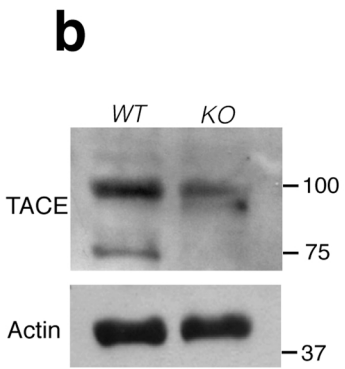
b
WT
KO
TACE
Actin
100
75
37

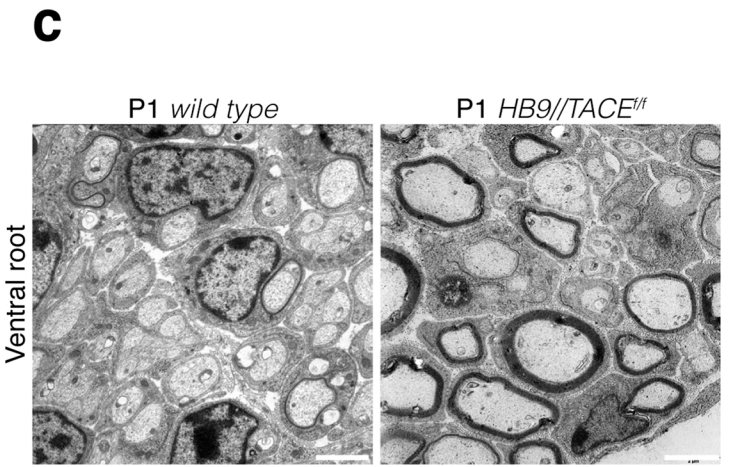
c
P1 wild type
P1 HB9//TACEf/f
Ventral root

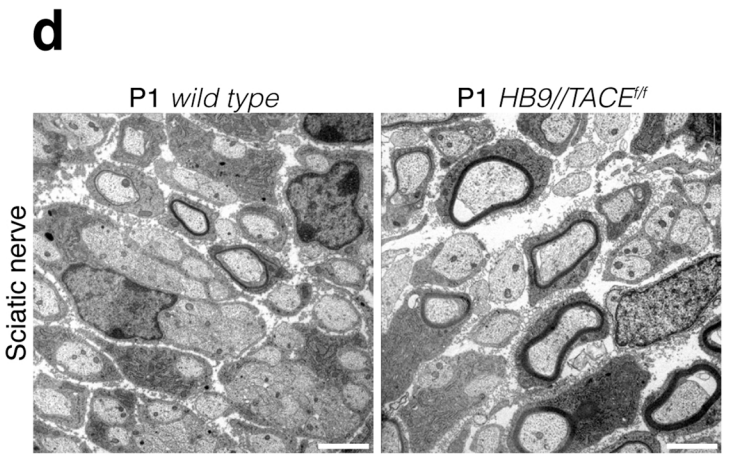
d
P1 wild type
P1 HB9//TACEf/f
Sciatic nerve

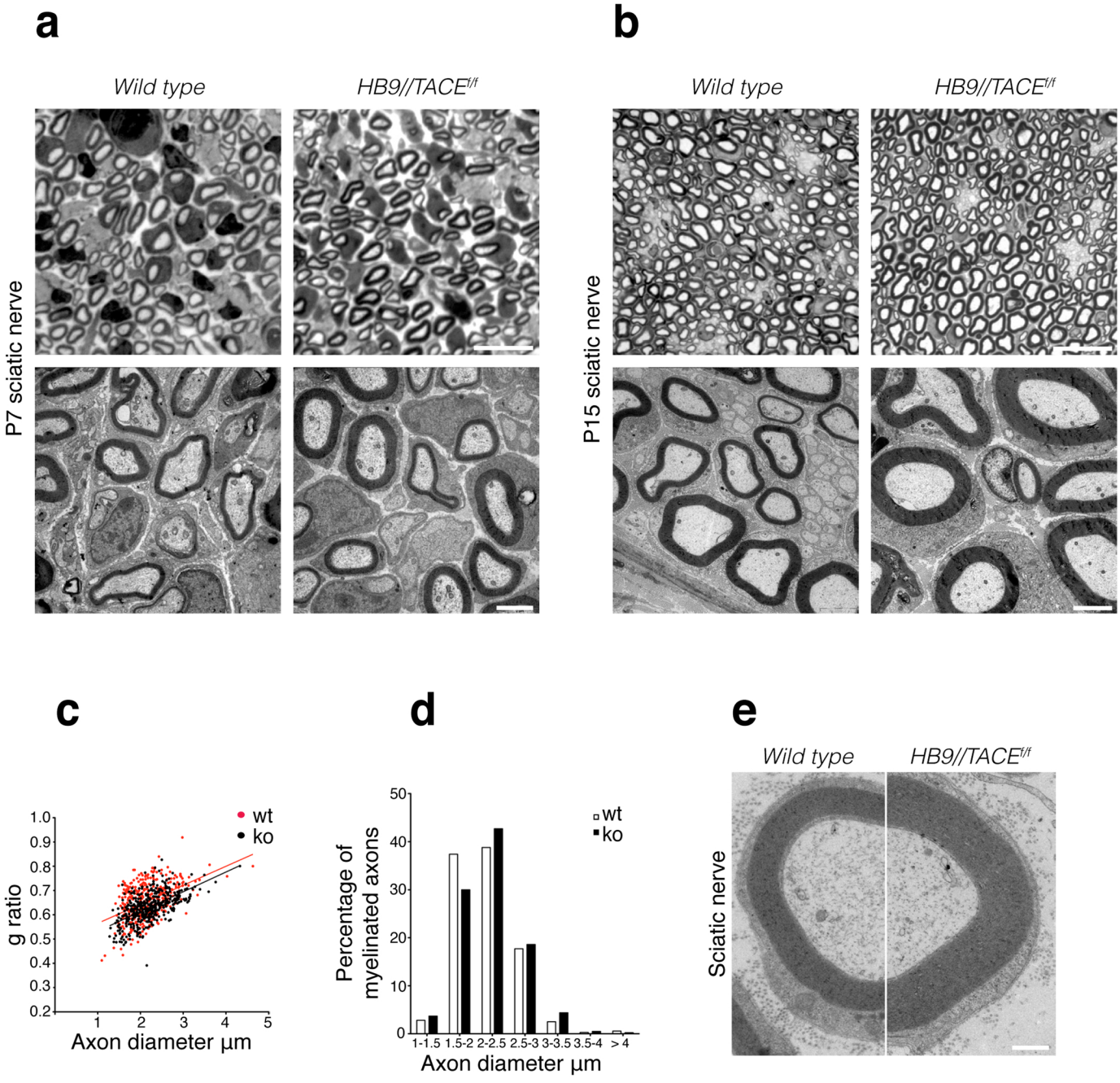
a
Wild type
HB9//TACEf/f
P7 sciatic nerve
b
Wild type
HB9//TACEf/f
P15 sciatic nerve
c
wt
ko
g ratio
1.0
0.9
0.8
0.7
0.6
0.5
0.4
0.3
0.2
1
2
3
4
5
Axon diameter µm
d
wt
ko
Percentage of myelinated axons
50
40
30
20
10
0
1-1.5
1.5-2
2-2.5
2.5-3
3-3.5
3.5-4
> 4
Axon diameter µm
e
Wild type
HB9//TACEf/f
Sciatic nerve

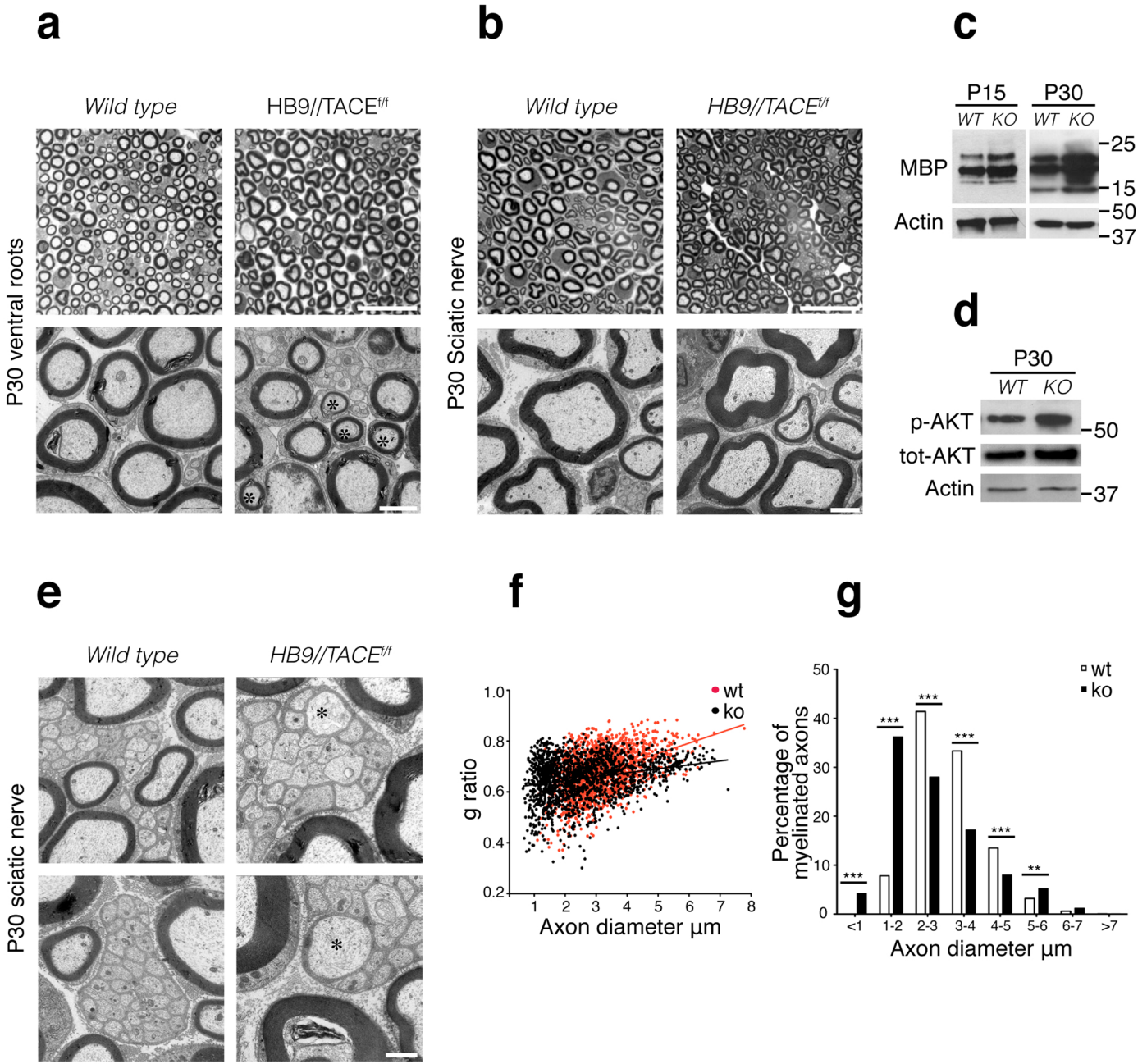
a
Wild type
HB9//TACEf/f
P30 ventral roots
b
Wild type
HB9//TACEf/f
P30 Sciatic nerve
c
P15
P30
WT KO
WT KO
MBP
Actin
25
15
50
37
d
P30
WT KO
p-AKT
tot-AKT
Actin
50
37
e
Wild type
HB9//TACEf/f
P30 sciatic nerve
f
wt
ko
g ratio
Axon diameter µm
g
wt
ko
Percentage of myelinated axons
Axon diameter µm
<1
1-2
2-3
3-4
4-5
5-6
6-7
>7

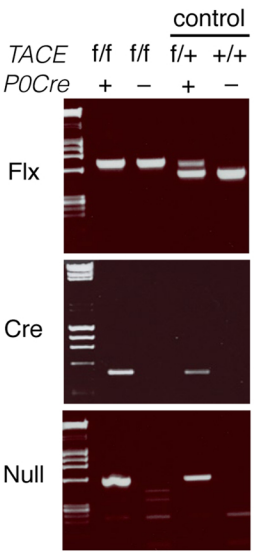
a
control
TACE f/f f/f f/+ +/+
P0Cre + − + −
Flx
Cre
Null

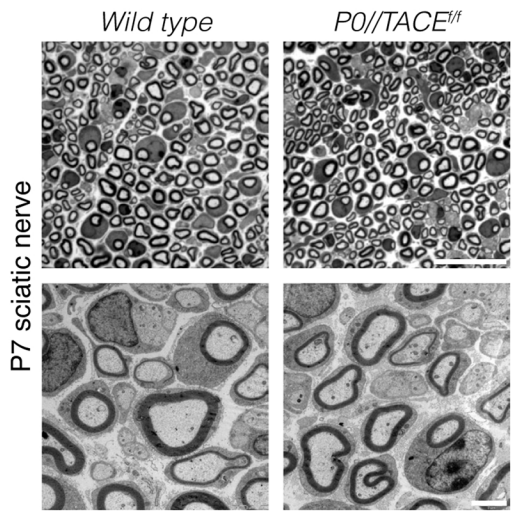
b
Wild type
P0//TACE f/f
P7 sciatic nerve

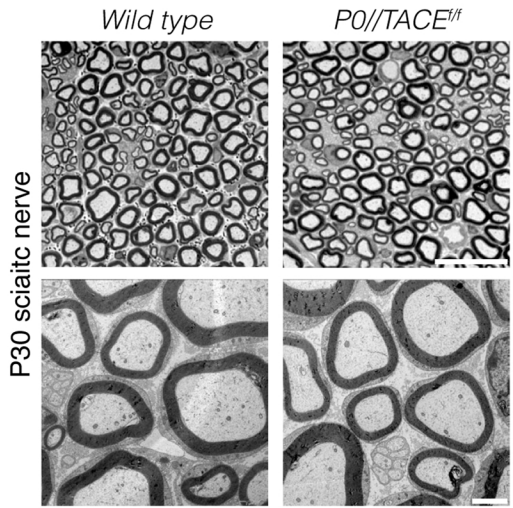
c
Wild type
P0//TACE f/f
P30 sciaitc nerve

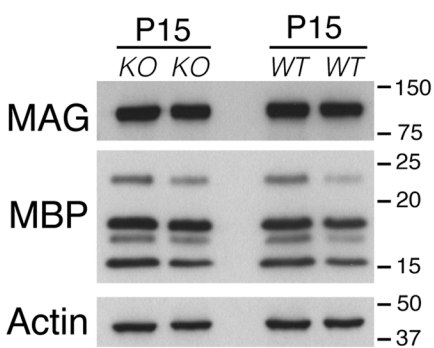
d
P15
KO KO
P15
WT WT
MAG
MBP
Actin
150
75
25
20
15
50
37

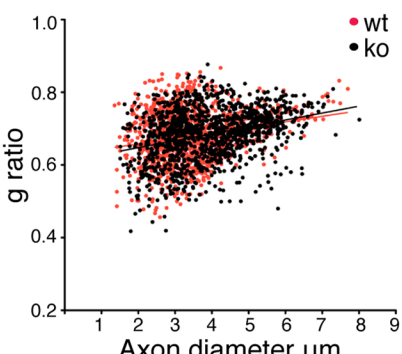
e
wt
ko
g ratio
1.0
0.8
0.6
0.4
0.2
1 2 3 4 5 6 7 8 9
Axon diameter µm

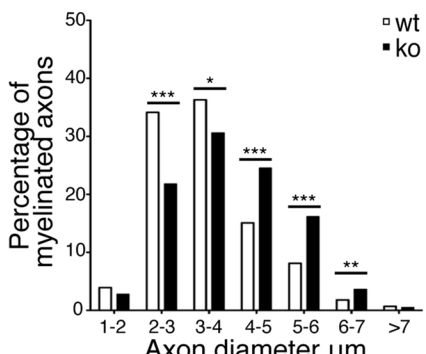
f
wt
ko
Percentage of myelinated axons
50
40
30
20
10
0
***
*
***
***
**
1-2 2-3 3-4 4-5 5-6 6-7 >7
Axon diameter µm

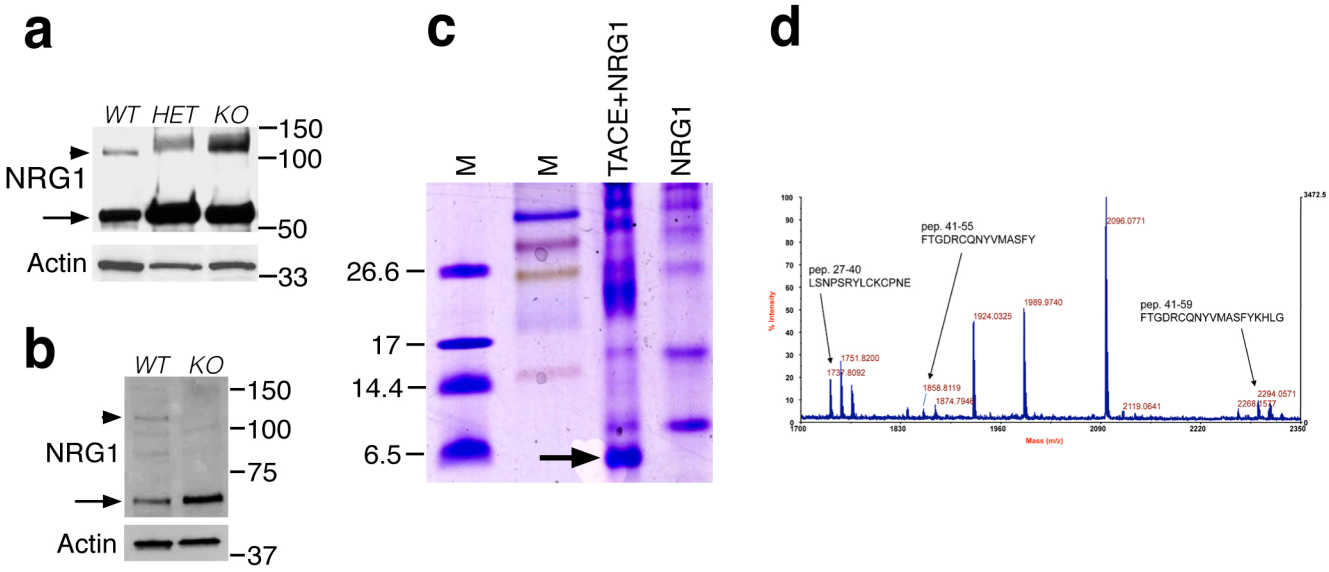
a
WT HET KO
NRG1
Actin
150
100
50
33
b
WT KO
NRG1
Actin
150
100
75
37
c
M
M
TACE+NRG1
NRG1
26.6
17
14.4
6.5
d
pep. 27-40
LSNPSRYLCKCPNE
pep. 41-55
FTGDRCQNYVMASFY
pep. 41-59
FTGDRCQNYVMASFYKHLG
% Intensity
Mass (m/z)

e
NRG1β1: TSHLVKCAEKEKTFCVNGGECFMVKDLSNPSRYLCKCPNEFTGDRCQNYVMASFYKHLGIEFMEAEELYQKRVLTITGICIALLVVGIMCVVAYC
α α β

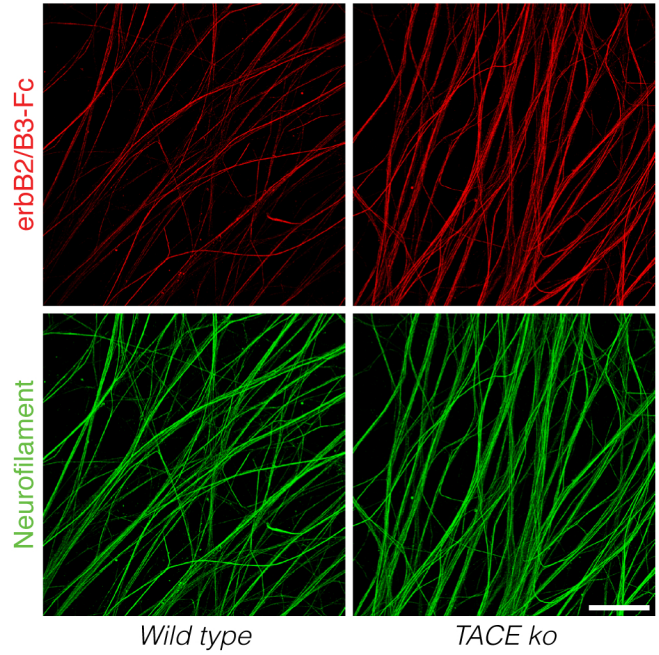
f
erbB2/B3-Fc
Neurofilament
Wild type
TACE ko

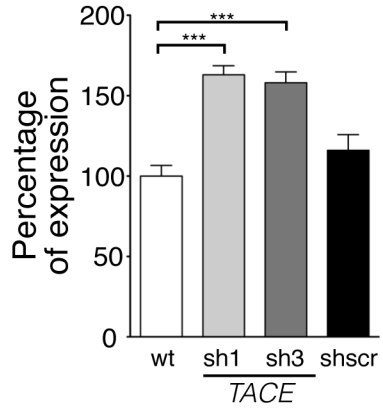
g
Percentage of expression
200
150
100
50
0
***
***
wt
sh1
sh3
shscr
TACE

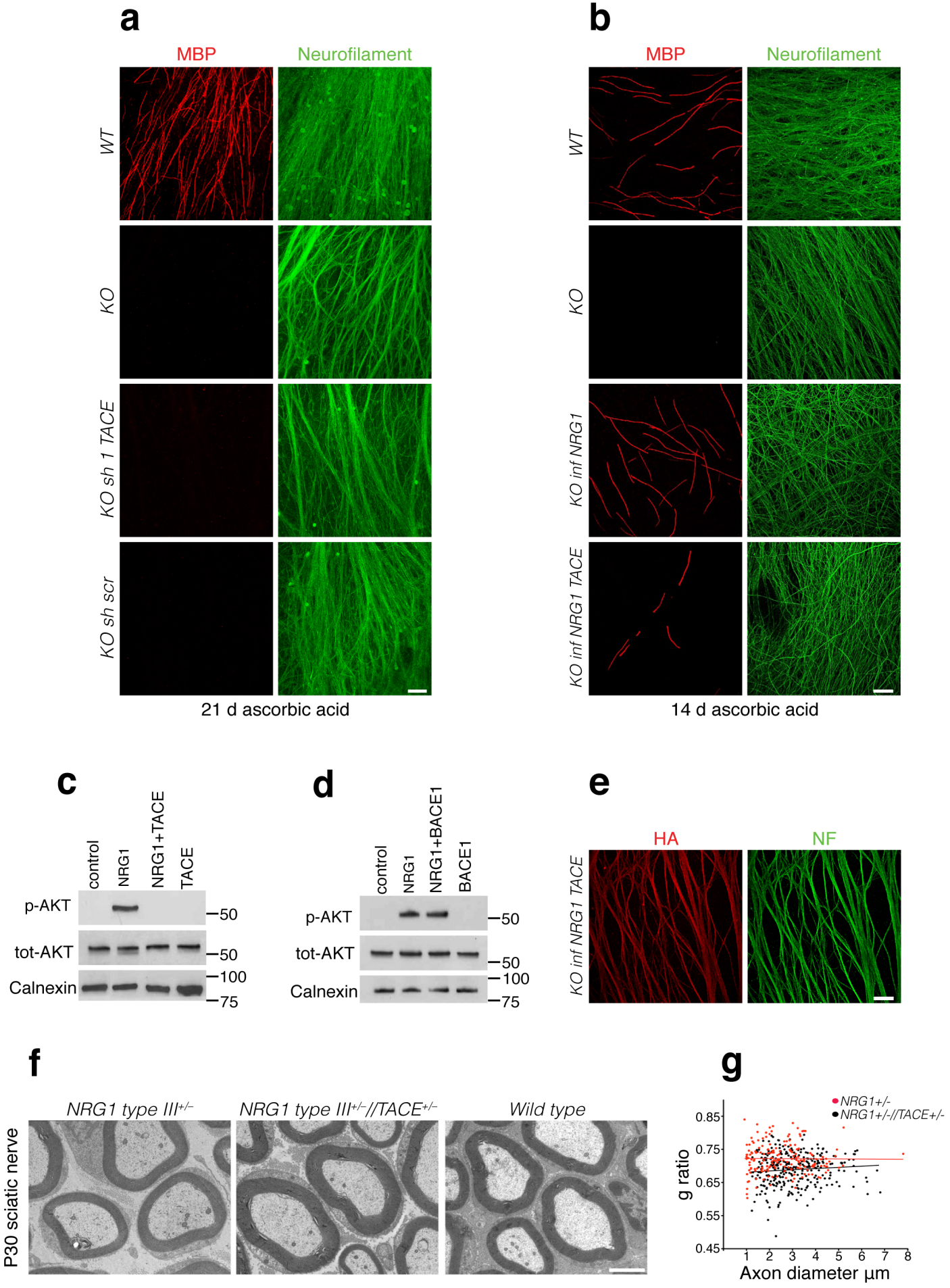
a
MBP
Neurofilament
WT
KO
KO sh 1 TACE
KO sh scr
21 d ascorbic acid
b
MBP
Neurofilament
WT
KO
KO inf NRG1
KO inf NRG1 TACE
14 d ascorbic acid
c
control
NRG1
NRG1+TACE
TACE
p-AKT
tot-AKT
Calnexin
50
50
100
75
d
control
NRG1
NRG1+BACE1
BACE1
p-AKT
tot-AKT
Calnexin
50
50
100
75
e
HA
NF
KO inf NRG1 TACE
f
NRG1 type III+/-
NRG1 type III+/-//TACE+/-
Wild type
P30 sciatic nerve
g
NRG1+/-
NRG1+/-//TACE+/-
g ratio
0.85
0.75
0.65
0.55
0.45
1
2
3
4
5
6
7
8
Axon diameter µm

Supplementary Information Titles

Please list each supplementary item and its title or caption, in the order shown below. Please include this form at the end of the Word document of your manuscript or submit it as a separate file.

Note that we do NOT copy edit or otherwise change supplementary information, and minor (nonfactual) errors in these documents cannot be corrected after publication. Please submit document(s) exactly as you want them to appear, with all text, images, legends and references in the desired order, and check carefully for errors.

Journal: Nature Neuroscience

Article Title:	ADAM 17/TACE inhibits Schwann cell myelination
Corresponding Author:	Carla Taveggia, Ph.D.

Supplementary Item & Number **(add rows as necessary)**	Title or Caption
Supplementary Figure 1	TACE is expressed in Schwann cells and DRG neurons.
Supplementary Figure 2	$P75^{NTR}$ but not Notch-1 is target of TACE shRNA lentiviruses.
Supplementary Figure 3	TACE activity is neuronal autonomous.
Supplementary Figure 4	TACE +/- sciatic nerves are normally myelinated.
Supplementary Figure 5	Abnormalities in P0Cre//$TACE^{flx/flx}$ mice.
Supplementary Figure 6	MALDI-TOF spectra of TACE cleavage sites of NRG1 type III.
Supplementary Figure 7	NRG1 levels are increased in TACE null DRG neurons.
Supplementary Figure 8	TACE ablation does not rescue myelination of NRG1 type III null neurons.
Supplementary Figure 9	Schematic model representing NRG1 type III shedding in myelination.
Supplementary Figure 10	Uncropped pictures of Western Blots in manuscript.
Supplementary Table 1	Morphometric analyses of wild type and TACE null mice.

ADAM17/TACE inhibits Schwann cell myelination

Rosa La Marca, Federica Cerri, Keisuke Horiuchi, Angela Bachi, M. Laura Feltri, Lawrence Wrabetz, Carl P. Blobel, Angelo Quattrini, James L. Salzer and Carla Taveggia.

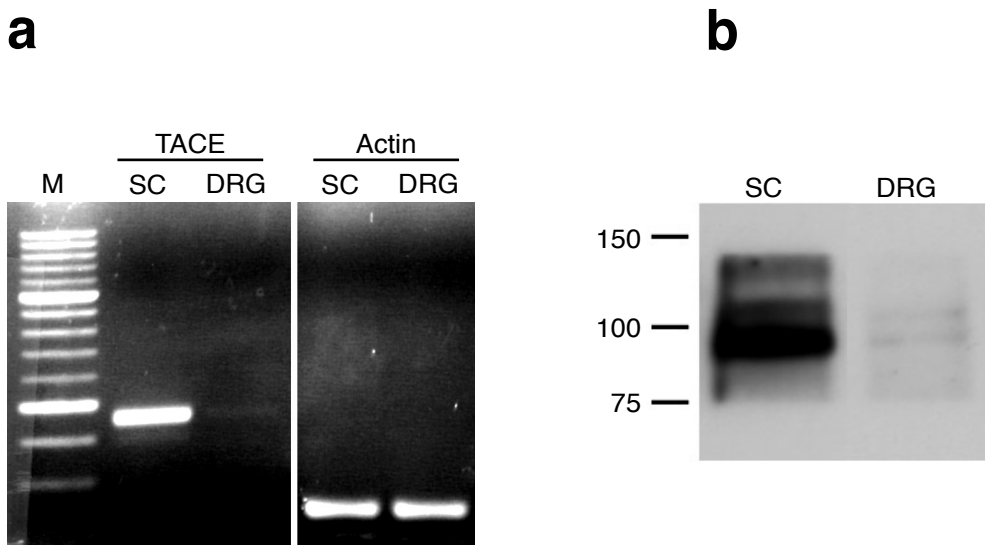

Supplementary Figure 1. TACE is expressed in Schwann cells and DRG neurons. RT-PCR (**a**) and Western blotting analyses (**b**), showing high level of TACE mRNA and protein expression in Schwann cells and lower levels in DRG neurons. Actin expression is a control for equal loading.

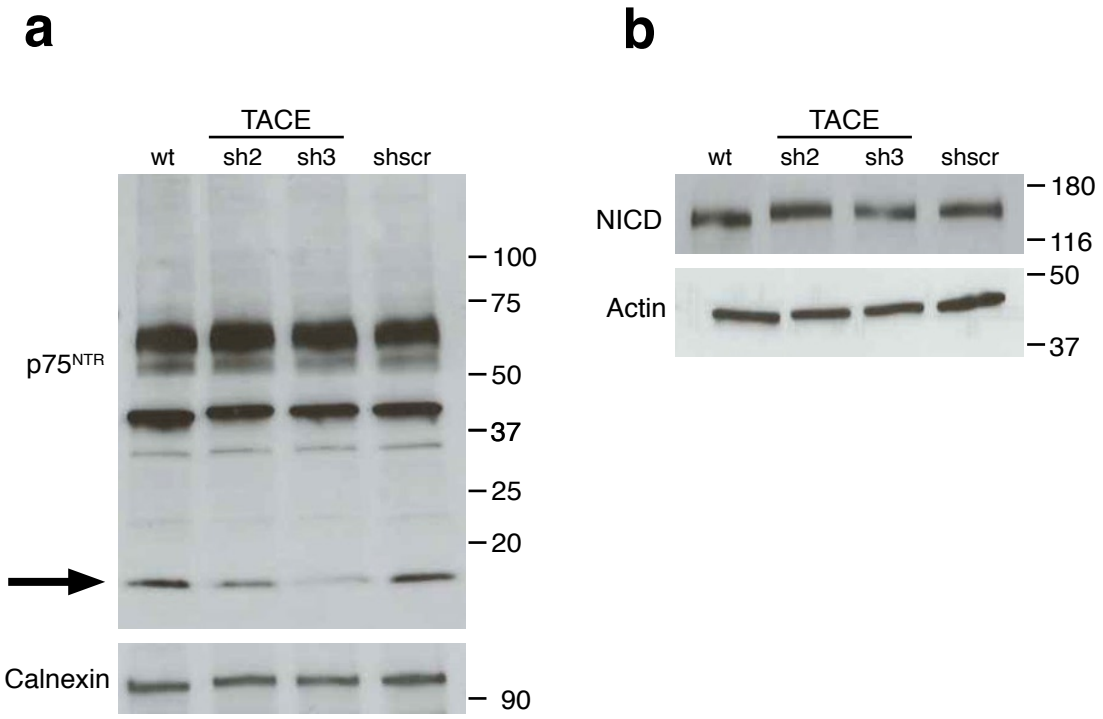

Supplementary Figure 2. p75^{NTR} but not Notch–1 is target of TACE shRNA lentiviruses. Cocultures of wild type DRG neurons infected with TACE sh2 and sh3 or shscr, purified of endogenous Schwann cells and grown with wild type not infected rat Schwann cells. Cultures were maintained in myelinating conditions for 14 days, and then lysed to determine p75^{NTR} (**a**) and Notch–1 cleavage (**b**) by Western Blotting analysis. As expected only p75^{NTR} cleavage is impaired in shTACE lentivirus infected cultures, but not Notch–1. The arrow in (**a**) indicates the product of p75^{NTR} processing[18].

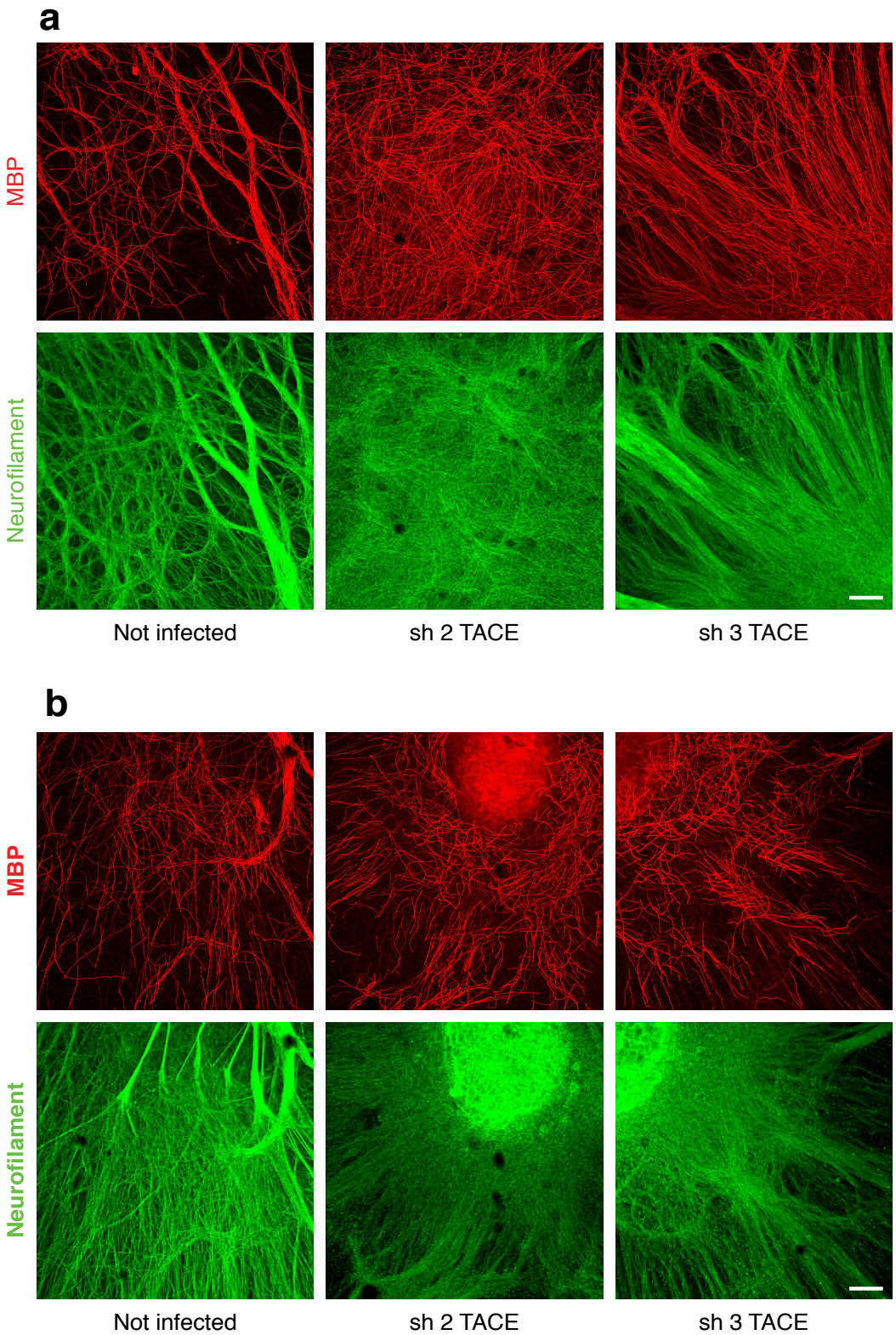

Supplementary Figure 3. TACE activity is neuronal autonomous.
(**a**) Cocultures of wild type DRG neurons infected with TACE sh2 and sh3, purified of endogenous Schwann cells and grown with wild type not infected rat Schwann cells. Cultures were maintained in myelinating conditions for 14 days, fixed and stained for the myelin protein MBP (rhodamine) and neurofilament (fluorescein). Numerous myelin segments are evident in sh TACE infected; fewer segments are present in control not infected cultures. Bar: 100 µm.
(**b**) Cocultures of purified wild type not infected mouse DRG neurons repopulated with wild type rat Schwann cells previously infected with TACE sh2 and sh3. Cultures were maintained in myelinating conditions for 21 days, fixed and stained for the myelin protein MBP (rhodamine) and neurofilament (fluorescein). No difference in myelination extent is present in infected versus not infected or scramble infected cultures. Bar: 100 µm.

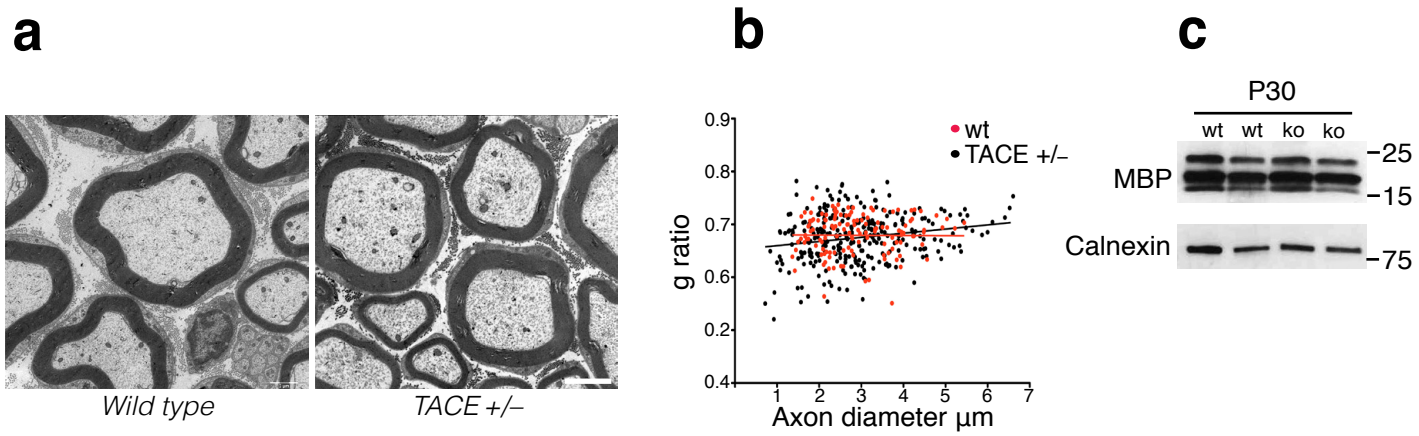

Supplementary Figure 4. TACE +/– sciatic nerves are normally myelinated.
(**a**) Ultrastructural analyses of wild type and P30 TACE +/– sciatic nerves. Wild type and TACE heterozygous mice are comparably myelinated. Bars: 2 µm. (**b**) *g* ratios as a function of axon diameter are identical in wild type (red line) and TACE +/– P30 sciatic nerve fibers (black line) mice (p = not significant). The graph represent the g ratio obtained from more than 200 myelinated axons (3 animals per genotype). (**c**) Lysates of wild type and TACE +/– P30 sciatic nerves were fractionated by SDS PAGE and blotted with antibodies to MBP and calnexin as loading control. No alteration in myelin protein expression is observed among wild type and null animals.

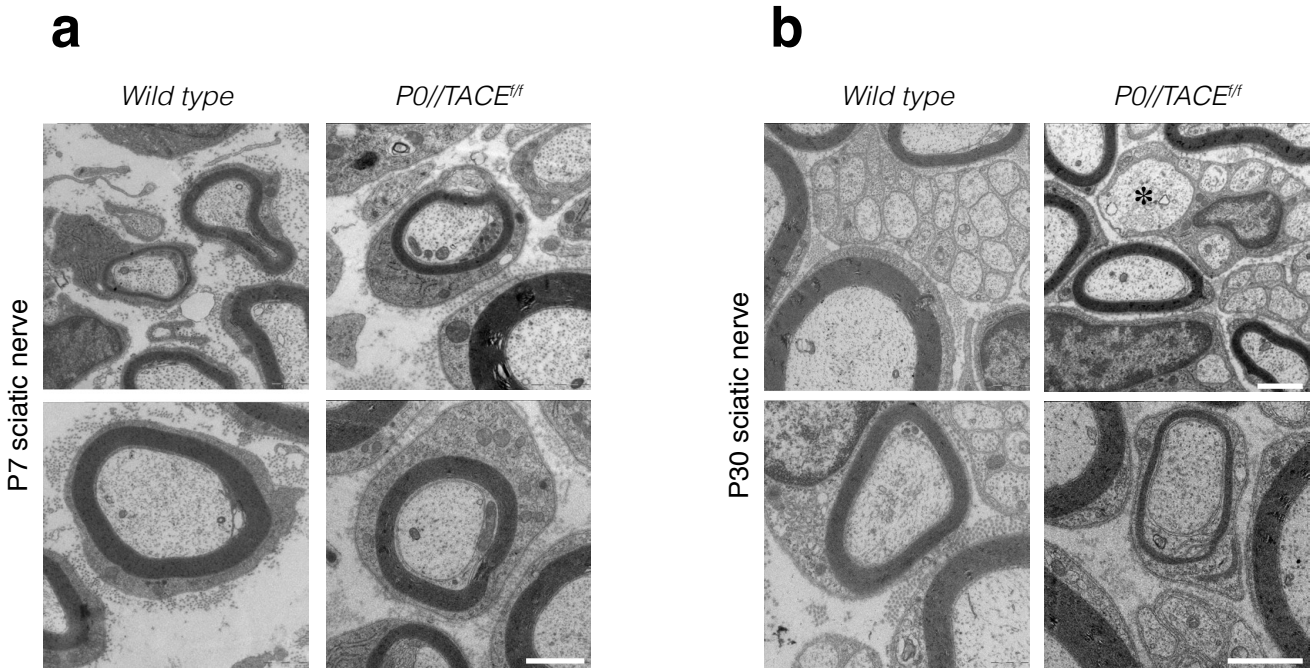

Supplementary Figure 5. Abnormalities in P0Cre//TACE$^{flx/flx}$ mice.
Ultrastructural analyses of P7 (**a**) and P30 (**b**) P0Cre//TACE$^{flx/flx}$ sciatic nerves. Mitochondria and vacuoles accumulate at both ages in the inner cytoplasmic collar of null animals but not in control wild type mice. Of note in **b**) the presence of large unsegregated and unmyelinated axons in a Remak bundles (asterisk). Bars: 1 µm.

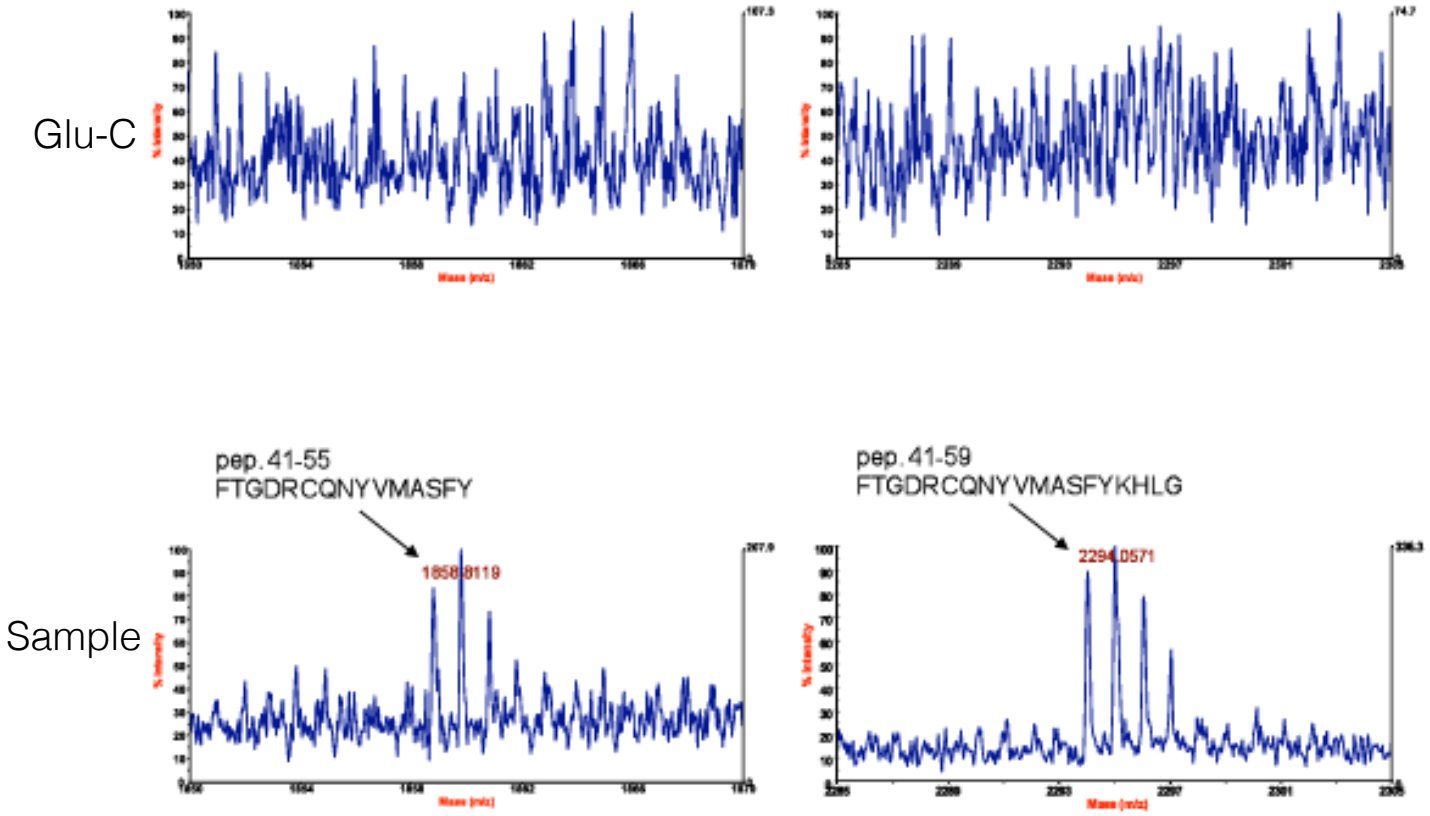

Supplementary Figure 6. MALDI-TOF spectra of TACE cleavage sites of NRG1 type III. Spectra generated by the Endopeptidase Glu-C alone (upper panels) and specific peaks identified upon digestion of NRG1 by TACE by the Endopeptidase Glu-C (lower panels).

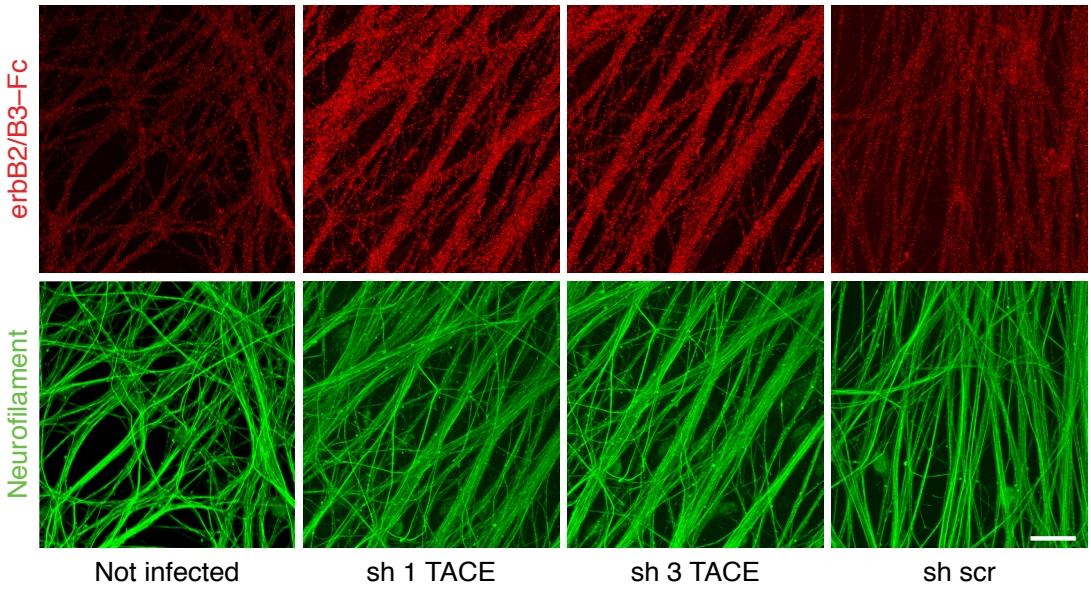

Supplementary Figure 7. NRG1 levels are increased in TACE null DRG neurons. Cultures of wild type DRG neurons or infected with TACE specific shRNA (sh1 and sh3) were incubated with erbB2/3–Fc and then fixed and visualized with rhodamine–conjugated anti–human Fc antibodies; neurofilament staining from the corresponding fields is shown (fluorescein). erbB2/3–Fc binds stronger to TACE null neurons compared to wild type neurons. Bar: 40 µm.

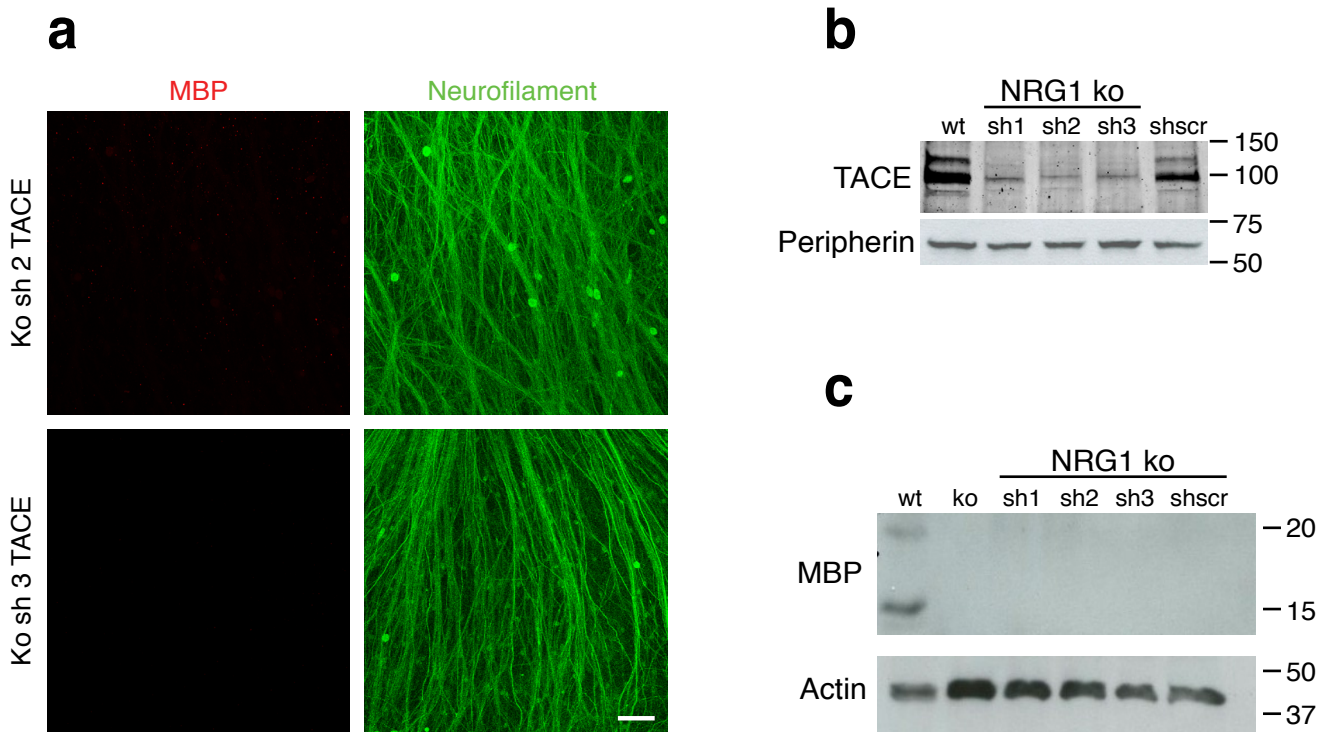

Supplementary Figure 8. TACE ablation does not rescue myelination of NRG1 type III null neurons.
(**a**) Cocultures of type III NRG1 null neurons infected with TACE specific shRNA (sh2 or sh3) were maintained in myelinating conditions together with wild type rat Schwann cells for 21 days; fixed and stained for MBP (rhodamine) and neurofilament (fluorescein). Bar: 50 µm. (**b**) Lysates of wild type uninfected or type III NRG1 null DRG neuronal cultures infected with TACE specific shRNA (sh1, sh2, sh3) or scramble sh RNAs (shscr) and grown with rat Schwann cells in myelinating conditions for 21 days, were probed for TACE and peripherin as loading control. TACE levels are downregulated in cocultures infected with TACE sh RNA, but not in wild type or scramble infected cultures. (**c**) Extracts prepared from the same cocultures were probed for MBP and actin as loading control. MBP is detected only in extracts of wild type cocultures, but not in type III NRG1 null neurons either infected or not.

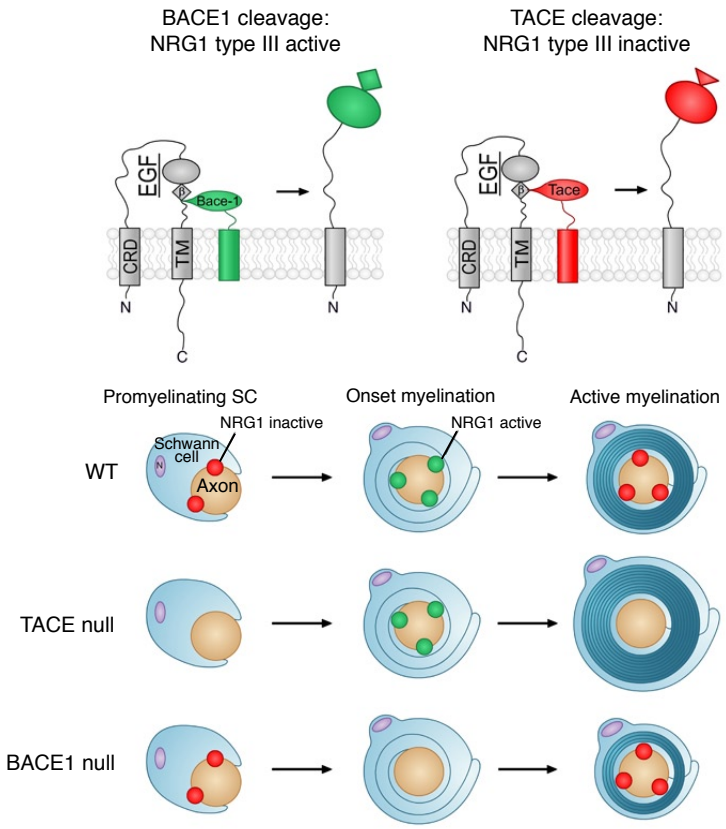

Supplementary Figure 9. Schematic model representing NRG1 type III shedding in myelination.

NRG1 activity is differentially regulated by TACE and BACE1 cleavage: TACE inactivates NRG1 type III, whereas BACE1 activates it. Based on our in vivo and in vitro data, TACE cleavage of NRG1 regulates the onset of myelination and the amount of myelin of the axons. Therefore, inhibition of TACE in neurons enhances the onset of myelination and results in hypermyelination, whereas, BACE1 inactivation leads to hypomyelination.

Figure 1a

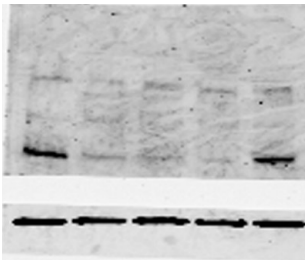

Figure 3b

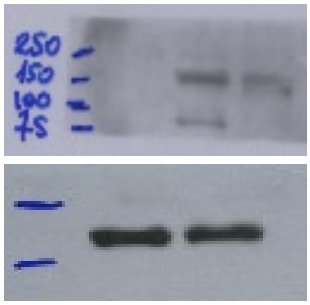

Figure 5d

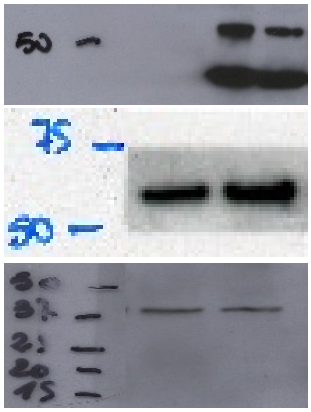

Figure 1d

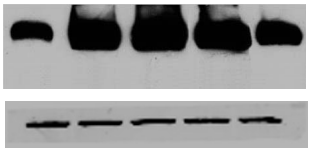

Figure 5c

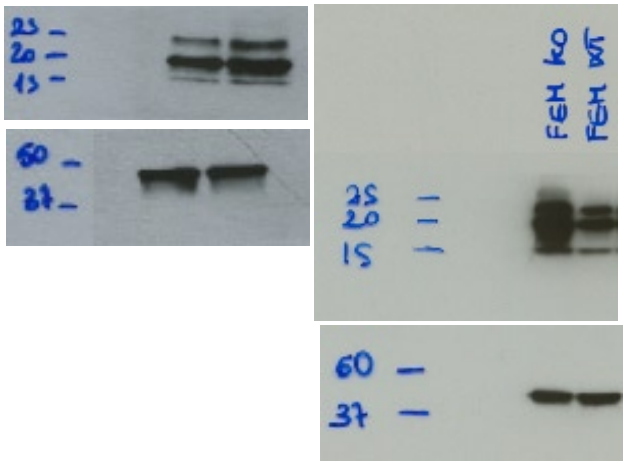

Figure 6d

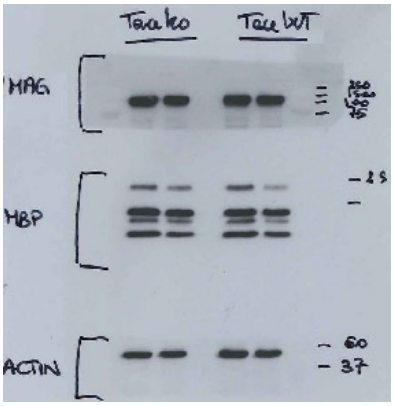

Figure 7a

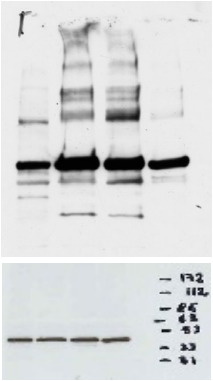

Figure 7b

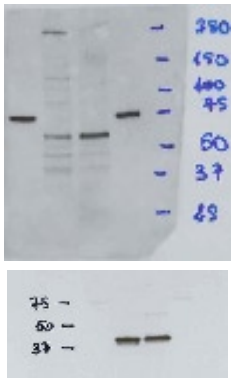

Figure 8c

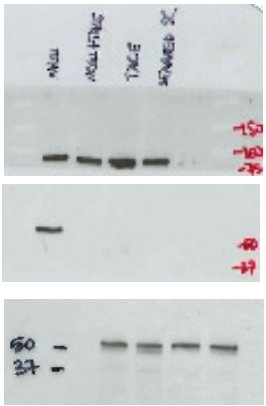

Figure 8d

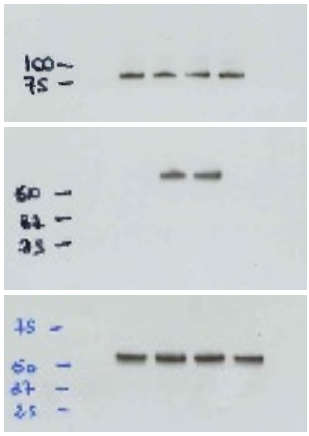

Supplementary Figure 10. Uncropped pictures of the Western Blots shown in the manuscipt

Supplementary Table 1. Morphometric analyses of *wild type* and *TACE*$^{-/-}$ mice

Total number of myelinated fibers per field in P1 sciatic nerve

		P
wild type	6.933 ± 0.5812	
HB9Cre//TACE$^{flx/flx}$	10.10 ± 0.6629	P=0.0039

***HB9Cre//TACE*$^{flx/flx}$ *g* ratios**

	wild type	*HB9Cre//TACE*$^{flx/flx}$	P
P7 sciatic nerve	0.68±0.006	0.65±0.005	P=0.0007
P30 sciatic nerve	0.68±0.002	0.65±0.002	P<0.0001

***HB9Cre//TACE*$^{flx/flx}$ P30 sciatic nerve number of myelinated fiber/diameter**

	wild type	*HB9Cre//TACE*$^{flx/flx}$	P
< 1 µm	0	72	P<0.0001
1-2 µm	133	621	P<0.0001
2-3 µm	703	479	P<0.0001
3-4 µm	566	296	P<0.0001
4-5 µm	229	137	P<0.0001
5-6 µm	54	89	P=0.0051
6-7 µm	10	21	NS
> 7 µm	1	1	NS

***P0Cre//TACE*$^{flx/flx}$ *g* ratios**

	wild type	*P0Cre//TACE*$^{flx/flx}$	P
P30 sciatic nerve	0.68±0.002	0.684±0.002	NS

P30 *P0Cre//TACE*$^{flx/flx}$ number of fiber/diameter

	wild type	*P0Cre//TACE*$^{flx/flx}$	P
1-2 µm	51	35	NS

2-3 µm	443	271	P<0.0001
3-4 µm	471	381	P=0.0363
4-5 µm	196	305	P<0.0001
5-6 µm	105	201	P<0.0001
6-7 µm	23	45	P=0.073
> 7 µm	9	6	NS

***NRG1 type III$^{+/-}$//TACE$^{+/-}$ g* ratios**

	wild type	*NRG1$^{+/-}$*	*NRG1 type III$^{+/-}$//TACE$^{+/-}$*	P
P30 sciatic nerve	0.68±0.003	0.72±0.003	0.69±0.002	P<0.0001

***TACE$^{+/-}$ g* ratios**

	wild type	*TACE$^{+/-}$*	P
P30 sciatic nerve	0.68±0.003	0.674±0.002	NS

Summary of the morphometric analyses performed in *wild type* and *TACE$^{-/-}$* mice. Indicated are the total number of myelinated fibers per field in P1 *HB9Cre//TACE$^{flx/flx}$* sciatic nerves (**Fig. 3**); *g* ratio values for P7 and P30 *HB9Cre//TACE$^{flx/flx}$* sciatic nerves (**Fig. 4** and **Fig. 5**); *g* ratio measurements for P30 *P0Cre//TACE$^{flx/flx}$* sciatic nerves (**Fig. 6**); *g* ratio values for P30 *NRG1 type III$^{+/-}$//TACE$^{+/-}$* sciatic nerves (**Fig. 8**); *g* ratio measurements of *P30 TACE$^{+/-}$* sciatic nerves (**Supplementary Fig. 4**). Reported are also the total number of myelinated fibers in P30 *HB9Cre//TACE$^{flx/flx}$* (**Fig. 4** and **Fig. 5**) and P30 *P0Cre//TACE$^{flx/flx}$* (**Fig. 6**) sciatic nerves, binned according to a specific diameter. Morphologic analyses were performed using NIH Image J. Leica QWin and Prism softwares.

Nature Neuroscience manuscript checklist NN-A33089B

Author: Please tick each of the points below to indicate that it has been addressed. Then sign at the bottom and either (1) upload as a Related Manuscript file, along with your other final manuscript files and License form, or (2) return it by fax (212-696-0978).

Special Considerations

- ☒ Please modify your figures as indicated on the attached PDF.
- ☒ **Two-letter abbreviations are not permitted; please spell out.**
- ☒ **Subheadings (in Results/Discussion) must fit onto one line in print—≤58 characters including spaces—and should refer to at least two paragraphs.**
- ☒ Figures: please indicate nature of error bars (*i.e.*, s.e.m. or s.d.) and magnitude of scale bars (in the figure itself or in the figure legend).
- ☒ Please ensure that figure panels are cited in order in the text, and that all are cited.
- ☒ Please ensure that references are cited in order in the text, and that all are cited. References order: main text, figure legends, tables, Online Methods.
- ☒ Ensure that **all** gene symbols used have been recognized by the appropriate nomenclature committee: for humans, the HUGO Gene Nomenclature Committee (http://www.gene.ucl.ac.uk/nomenclature/); for mice, the Mouse Genome Database (http://www.informatics.jax.org/). For other organisms, refer to http://www.ncbi.nih.gov/entrez.
- ☒ Microarray data must be submitted to GEO or ArrayExpress and accession codes given in the paper. Please ensure data will be public as of the paper's online publication date.
- ☒ Please confirm that the paper complies with Nature Publishing policy concerning image integrity (see http://www.nature.com/authors/editorial_policies/image.html).

Results

- ☒ Avoid describing figures—this should be kept to the figure legends.

Text—General Points

- ☒ Discuss previous findings (established knowledge) in the present tense; discuss findings of this paper in the past tense ("We found..."; "These cells showed...")
- ☒ Use the active, not passive, voice throughout the main body of the text and in the Methods section. For example, (i) is preferable to (ii) in the following example:
  (i) We obtained aliquots of 5–30 ml of peripheral blood from each family member.
  (ii) 5–30 ml of peripheral blood were obtained from each family member.
- ☒ Define all abbreviations and symbols the first time they are used.
- ☒ We do not permit specific mention of other authors by name; use citation numbers only.
- ☒ Use the style (**Fig. 1a,c,f**), (**Fig. 2a–c**), (**Figs. 2** and **3**), (**Fig. 1** and **Table 2**) to refer to figures in the text (parentheses, commas and en dashes not bold). Figure citations in the text should not refer to specific parts of display items (such as gel lanes, tissue sections, arrows etc.). Avoid the construction "**Figure 1** shows that...."

Text—Formatting

- ☒ Throughout text AND figures and tables, please use the 'en-dash' (–), which is slightly wider than a hyphen (-), for negative and minus signs and number ranges. On a PC: Ctrl then minus key; on a Mac, Option then minus key.

- ☒ Genes and genotypes (and all constructs that are DNA, cDNA or RNA) must be *italicized* throughout text and figures and given the correct designation according to the species (see above).
- ☒ Refer to mutants as $DAT^{-/-}$ (note that these are superscript en-dash symbols), not as "–/–" or "KO".
- ☒ Make sure all Greek letters (α, β, γ, μ) and mathematical symbols (°, × (for scientific notation and magnification), ±) are in Symbol font. If using Microsoft Word, use Insert > Symbol to ensure the symbols are not lost in typesetting.

Author Contributions

- ☒ Each article must contain a brief statement specifying the individual contributions of each coauthor to this work. (An example: "A.M. conducted the xxx experiments and wrote the manuscript; B.v.R. prepared the mutant proteins and contributed to the *in vitro* studies; C.-S.Q. conducted the data analyses; L.J.A. supervised the project..." etc.)

Reference List

- ☒ Cite all references in numerical order as follows: main text (Introduction, Results, Discussion), figure legends, tables, Methods.
- ☒ No more than **50**; format the citations as[1,2,3–5].
  - Journal article example: Jennings, C.J., Mitsu, B. & Carr, K.R. Where to publish your research. *Proc. Natl. Acad. Sci. USA* **73**, 208–212 (1996).
  - Book chapter example: Wenz, C. *et al.* Scientific publishing takes the cake. in *The Production Nightmare* 2nd edn. Vol. 56 (eds. Whittock, K. & Raphe, N.) 222–333 (Oxford Univ. Press, New York, 1935).
- ☒ Only papers that have been published or are in press should be in the reference list. Papers in preparation or submitted should be cited parenthetically in the text (as 'unpublished data' or 'data not shown'). Please cite unrefereed, unpublished abstracts in the text in the form (A.B. Author & C.D. Author, *Soc. Neurosci. Abstr.* 243.3, 1996).

Figure Legends

- ☒ Please limit figure legends to a physical description, and move methods and results information to the appropriate text section. **No legend should exceed 250 words.**

Supplementary web material

- ☒ Each piece of Supplementary Information must be given a unique name and be cited by name, in numerical order, in the text.
- ☒ Provide a tabular list (electronic copy), named 'SI Guide', of all supplementary items and provide a brief, specific title for each supplementary table, figure, video or audio. Please use the 'Supplementary Information Titles' template at the end of this document; you may fill the table in and submit as a separate file or include the table at the end of your main manuscript text file. Full captions should still be included at the end of the Word document of your main manuscript.
- ☒ Please submit supplementary figures, tables and text as PDFs, and preferably as one combined PDF (with the pieces in the order figures, tables, text). Include the legend on the same page as each supplementary figure.
- ☒ Please list the title and authors of your paper at the top of the first piece of Supplementary Information.
- ☒ Personal or outside websites should not be called 'Supplementary Information'; this term refers only to supplementary items posted on Nature Neuroscience website.

Author signature: ....Carla Tavegne..... **Date:** ..April 7, 2011

Print Form

LICENSE TO PUBLISH

nature publishing group

Manuscript #: NN-A33089B [Nature Neuroscience] ("the Journal")

Title of the contribution:

ADAM17/TACE inhibits Schwann cell myelination ("the Contribution")

Author(s):

Rosa La Marca, Federica Cerri, Keisuke Oriuchi, Angela Bachi, M. Laura Feltri, Lawrence Wrabetz, Carl P. Blobel, Angelo Quattrini, James L. Salzer and Carla Taveggia ("the Authors")

To: Nature America Inc, trading as Nature Publishing Group ("NPG")

1. In consideration of NPG agreeing to publish the Contribution the Authors grant to NPG for the full term of copyright in the Contribution and any extensions thereto, subject to clause 2 and 3 below, the exclusive license (a) to publish, reproduce, distribute, display and store the Contribution in all forms, formats and media whether now known or hereafter developed (including without limitation in print, digital and electronic form) throughout the world, (b) to translate the Contribution into other languages, create adaptations, summaries or extracts of the Contribution or other derivative works based on the Contribution and exercise all of the rights set forth in (a) above in such translations, adaptations, summaries, extracts and derivative works and (c) to license others to do any or all of the above.

2. Ownership of copyright remains with the Authors, and provided that, when reproducing the Contribution or extracts from it, the Authors acknowledge first and reference publication in the Journal, the Authors retain the following non-exclusive rights:
   a) To reproduce the Contribution in whole or in part in any printed volume (book or thesis) of which they are the author(s).
   b) They and any academic institution where they work at the time may reproduce the Contribution for the purpose of course teaching.
   c) To post a copy of the Contribution as accepted for publication after peer review (in Word or Tex format) on the Authors' own web site or institutional repository, or the Authors' funding body's designated archive, six months after publication of the printed edition of the Journal, provided that they also give a hyperlink from the Contribution to the Journal's web site.
   d) To reuse figures or tables created by them and contained in the Contribution in other works created by them.

3. In consideration of NPG agreeing to publish the Contribution, the Authors also grant to NPG for the full term of copyright and any extensions thereto the same rights, that have been granted in respect of the Contribution as set out in clause 1 above, in the Supplementary Information but on a non-exclusive basis.

4. NPG acknowledges that an earlier version of and/or work or material contained within the Contribution may have been submitted to a pre-print service such as arXiv or *Nature Precedings* (in accordance with that service's standard license terms).

5. The Authors warrant and represent that:
   a) The Authors are the sole authors of and sole owners of the copyright in the Contribution. If the Contribution includes materials of others, the Authors have obtained the permission of the owners of the copyright in all such materials to enable them to grant the rights contained herein. Copies of all such permissions are attached to this license.
   b) All of the facts contained in the Contribution are true and accurate.
   c) The Author who has signed this Agreement below has full right, power and authority to enter into this Agreement on behalf of all of the Authors.
   d) Nothing in the Contribution is obscene, defamatory, libelous, violates any right of privacy or infringes any intellectual property rights (including without limitation copyright, patent or trademark) or any other human, personal or other rights of any kind of any person or entity or is otherwise unlawful.
   e) Nothing in the Contribution infringes any duty of confidentiality which any of the Authors may owe to anyone else or violates any contract, express or implied, of any of the Authors, and all of the institutions in which work recorded in the Contribution was carried out have authorized publication of the Contribution.

6. The Authors authorize NPG to take such steps as it considers necessary at its own expense in the Authors' name and on their behalf if it believes that a third party is infringing or is likely to infringe copyright in the Contribution including but not limited to taking proceedings.

7. The Authors hereby consent to the inclusion of electronic links from the Contribution to third-party material wherever it may be located.

8. This Agreement shall be governed by the laws of the State of New York without reference to its conflict of laws principles and by the Federal laws applicable therein.

Signed for and on behalf of the Authors: Carla Taveggia Date: April 7, 2011

Please print name: CARLA TAVEGGIA

Address: Division of Neuroscience and INSPE
San Raffaele Scientific Institute
via Olgettina 58, 20132 Milan, ITALY